Lung Cancer and Its Early Detection Using Biomarker-Based Biosensors

ARTICLE *in* CHEMICAL REVIEWS · JULY 2011

Impact Factor: 46.57 · DOI: 10.1021/cr100420s · Source: PubMed

2 AUTHORS:

Sunil Kumar Arya
Institute of Microelectronics
71 PUBLICATIONS **1,942** CITATIONS
SEE PROFILE

Shekhar Bhansali
Florida International University
174 PUBLICATIONS **2,286** CITATIONS
SEE PROFILE

CHEMICAL REVIEWS

REVIEW

pubs.acs.org/CR

Lung Cancer and Its Early Detection Using Biomarker-Based Biosensors

Sunil K. Arya* and Shekhar Bhansali*

Bio-MEMS and Microsystem Lab, Department of Electrical Engineering, University of South Florida, 4202 East Fowler Avenue, ENB 118, Tampa, Florida 33620, United States

CONTENTS

1. INTRODUCTION

1.1. Lung Cancer

Cancer, one of the most life-threatening diseases, has more than 200 distinct types associated with it, affecting over 60 human organs. More than 90% of all cancer-related deaths occur from metastasis of the primary cancer tumor.[1] The early stages of cancer development carry the maximum potential for therapeutic intervention. Therefore, detecting premalignant or premetastatic malignant tumors when they are still confined within organ(s) is critical to enable effective treatment and improving survival rate.[1d] Among all cancers, lung cancer continues to be the most prevalent and life threatening globally. The disease has a severe impact on the quality of life, due to reduced oxygenation levels and a higher incidence of metastasis due to high blood flow in the lungs. It affects more than a million people worldwide and accounts for about 25% of all cancer deaths.[2]

Lung cancer is classified into two major groups: small cell lung carcinoma (SCLC) and nonsmall cell lung carcinoma (NSCLC). NSCLC is sometimes treated with surgery, while SCLC usually responds better to chemotherapy and radiation therapy. Small cell lung carcinoma can be further divided into three categories: small cell carcinoma, mixed small cell/large cell carcinoma, and combined small cell carcinoma (which also has components of squamous cell and/or adenocarcinoma). Major histologic types of NSCLC include squamous cell carcinoma (SCC), adenocarcinoma, bronchoalveolar carcinoma (BAC), and large cell carcinoma.[3]

1.2. Causes, Genetic Changes, and Traditional Screening of Lung Cancer

Tobacco smoking, exposure to environmental pollutants, second-hand smoke, and industrial substances like asbestos, radon, and arsenic are major causes of lung cancer.[3a,4] Epidemiological studies have shown that genetic factors also contribute to the risk of developing lung cancer.[3a,4] There are many challenges in the diagnosis of lung cancer, as it is often silent early in its course, and symptoms like shortness of breath, coughing, and weight loss are usually nonspecific. Thus, in most cases, lung cancer is diagnosed at an advanced stage when treatment outcomes are unfavorable.[5] Despite the advances made in diagnosis and treatment in the last few decades, the prognosis of lung cancer is still very poor. Lung cancer continues to have a high morbidity, with a 5 year survival rate of 60% at best.[3b,5a,6] Hence, there is a need for sensitive and reliable tools for preclinical diagnosis of lung cancer.

For cancer detection, it is important to understand its complexity, as no single gene is universally altered and the modification patterns of genes change within tumors at the same site.[1a,7] Cancer is a multistep process characterized by the accumulation of successive molecular, genetic, and epigenetic abnormalities. The genetic and molecular alterations such as gene mutation, microsatellite alteration, and promoter hypermethylation occur during the development and progression of cancer.[6,8] These

Received: December 9, 2010
Published: July 20, 2011

Table 1. Gene-Based Potential Biomarkers in Lung Cancer Detection[a]

groups	type of genes
chromosomal changes	deletion of the short arm of chromosome 3 (3p)
hypermethylation	serine protease family member-trypsinogen IV (PRSS3)
	tissue inhibitor of metalloproteinase (TIMP)-3
	death associated protein (DAP)-kinase
	P16, FHIT
genetic changes	K-ras, P53

[a] Adapted with permission from ref 2. Copyright 2004 BMB Reports.

alterations can be permanent, irreversible, or dynamic and can result in gain or loss in gene functioning.[9] In Table 1, some gene-based biomarkers in lung cancer detection are classified into groups based on change type.

Common genetic abnormalities in lung cancers include the loss of heterozygosity (LOH), genomic instability detected as microsatellite instability (MSI), and promoter hypermethylation in tumor suppressor genes.[2,8a,8c,10] It has been shown that microsatellite alteration and promoter hypermethylation are potential diagnostic markers for lung cancer.[11] Hsu et al. selected a panel of genetic and epigenetic markers and investigated microsatellite instability of D9S942, loss of heterozygosity of D9S286, D9S942, GATA49D12, and D13S170, and methylation of *p16INK4a* and *RARβ* in cytologically negative sputum and lung tumor tissues using a fluorescence technique. Their results showed sensitivity of 82%, specificity of 75%, and concordance of 79% between matched tumor and sputum samples.[8a]

Traditionally, abnormal chest imaging and/or nonspecific symptoms have led to the suspicion of lung cancer. To confirm the diagnosis, test have been done, including CT (computerized tomography, computerized axial tomography, or CAT) scan, low-dose helical CT scan (or spiral CT scan), magnetic resonance imaging (MRI) scan, positron emission tomography (PET) scan, and bone scans.[1b,3a,12] However, in the early stages of lung cancer, these tests have lacked the resolution to detect nascent sub-mm sized tumors and tend to be inconclusive. Sputum cytology, bronchoscopy, needle biopsy, etc.,[1b,3a,12] are prone to sampling and location/resolution errors and have led to similar challenges in early stage tumors.

Lung cancer has also been screened via biochemical screening. As an example, studies by Kuhn et al. demonstrated that the activity of cathepsin D in the fluid from bronchial lavage can be used for screening of bronchogenic carcinoma.[13] The biochemical approach offered an attractive alternative to address the shortcomings of present techniques and to improve lung cancer management and survival. Additionally, the sensitivity of electrochemical techniques has facilitated development of sensitive and specific screening tools for point-of-care detection and thus made the technique an integral part of early diagnosis strategies.

1.3. Lung Cancer Biomarkers

In cancer, as tumors develop, the cells or the organs release numerous DNA, proteins, and metabolites. The levels of these are associated with the stages of tumors and can therefore be used as biomarkers for screening and clinical diagnosis of cancer.[3b,8c,10] New and emerging genomic, proteomic, and metabolic studies involving biomarkers and pathways continue to be under investigation for better understanding of the disease, as well as for the discovery of potential genomic, proteomic, and metabolic biomarkers.[1b,d,7,14] The detection of biomarkers is the preferred approach for detecting/tracking lung cancer because of their unique association with genomic changes in cancer cells and with the disease process.[1c,10] Greater understanding of the disease process will enable biomarker detection to become the focal point of the therapeutic process by not only helping to identify who may be susceptible to cancer, but in some cases possibly also suggesting the likely timeline to susceptibility and the optimal time point for intervention.

Genetics-based cancer biomarkers utilize DNA arrays, polymerase chain reaction (PCR), reverse transcriptase polymerase chain reaction (RT-PCR), DNA sequencing, fluorescent in situ hybridization (FISH), etc., to detect the genetic alterations occurring in the cancerous state. On the other hand, proteomic techniques commonly include mass spectrometry, enzyme-linked immunosorbent assay, and immunohistochemistry, etc., and utilize these tools to discover novel cancer biomarkers and validate them in clinical trials,[2] while metabolic assays rely on liquid chromatography. Although genomic studies (epigenetic and genetic alterations) have provided valuable information on lung cancer molecular biology, the proteomic approach has opened a new window into the pathogenesis of lung cancer, as the phenotype of a cell is determined by proteins and cannot be predicted by genomics alone. Genetics require DNA extraction from tumor cells that are not easily obtained by noninvasive methods, whereas proteomics does not necessarily need a direct access to tumor cells. Proteins can easily and noninvasively be obtained from various sources such as blood, sputum, urine, or other bodily fluids.[15] Further, despite the significant advances in genomics and genetics-based biomarker discovery, there is still no novel cancer specific biomarker in clinical uses. DNA-based biomarkers are known to have potential as lung cancer biomarkers, but no biomarker has shown adequate sensitivity, specificity, and reproducibility to establish its direct association with lung cancer.[2] On the other hand, development of protein based biomarkers (specific proteins detected in abnormal amounts in the blood of cancer patients[1a]) for cancer diagnosis has increased significantly in recent years, and metabolite studies are currently under development to facilitate complete understanding of the disease process with associated biomarkers. Figure 1 schematically illustrates the workflow of the lung cancer biomarker discovery process.

Biomarkers detected in this process can be produced either by the tumor or by the body in response to the presence of a cancer tumor. Biomarkers can be broadly divided into DNA/genetic-based biomarkers, such as hypermethylation of promoters and mutation in the K-ras, p53 region of chromosomes, or protein/proteomics-based biomarkers such as carcinoembryonic antigen (CEA), neuron-specific enolase (NSE), etc. Both of these types can be detected in tumor cells, blood, sputum, urine, or other body fluids of cancer patients.[1b−d] In sputum, cancerous cells coming from cancer sites are a major source of proteins. Sputum is one of the most commonly utilized biological material to detect lung cancer cells in a noninvasive manner.[3a] Additionally, biomarkers from urine can also be easily obtained and utilized for noninvasive screening. Using proteomic techniques, Tantipaiboonwong et al. have investigated urinary protein markers and found that urine samples in lung cancer patients exhibit major differences at 14 kDa and in the range of 28−42 kDa, where protein bands with higher intensity than in normal urine samples

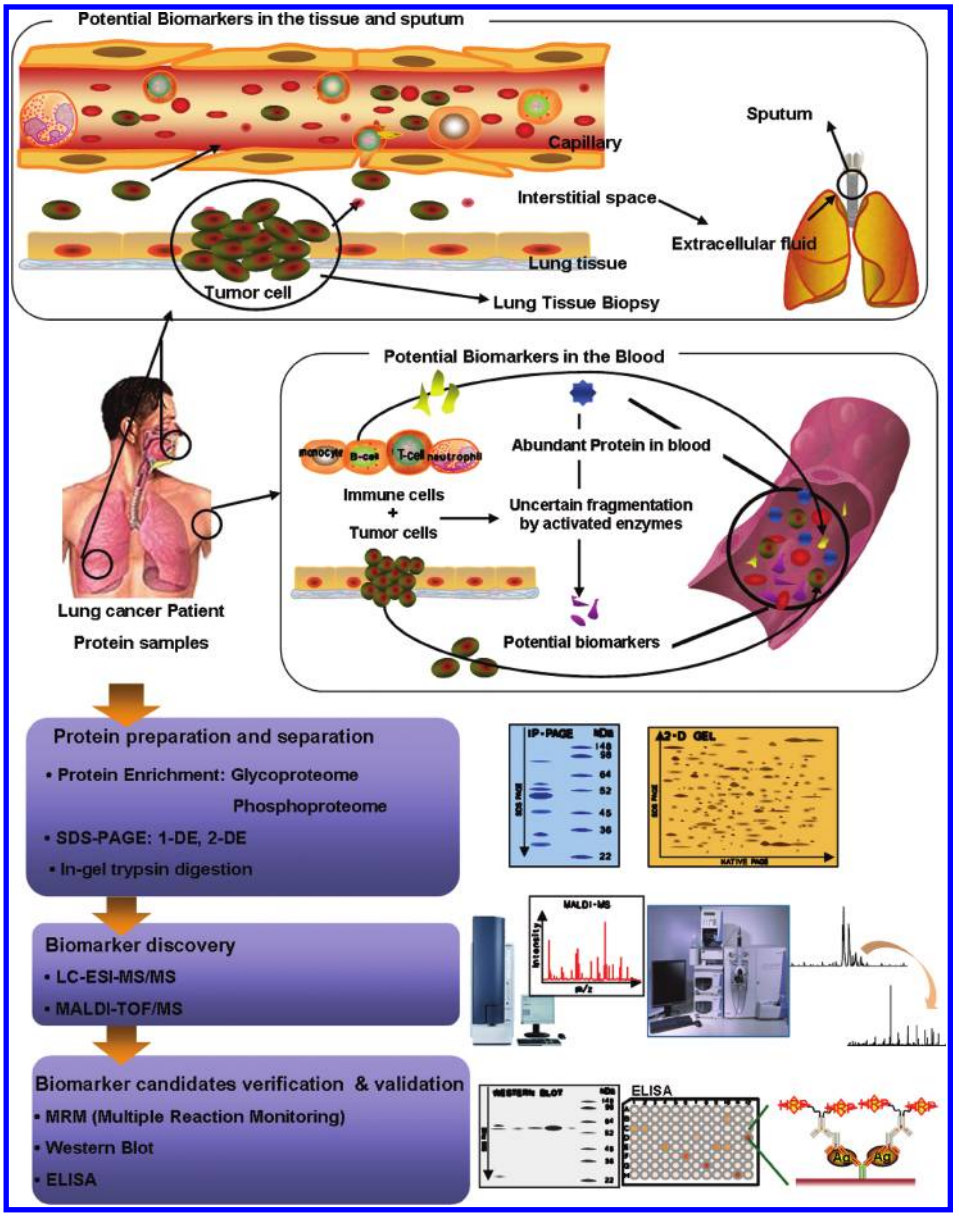

Figure 1. Schematic workflow of lung cancer biomarker discovery. Reprinted with permission from ref 2. Copyright 2004 BMB Reports.

(the controls) were found. In addition, urine samples of lung cancer patients had less protein at 50 kDa than controls. Further, they found that CD59 glycoprotein, transthyretin (TTR), GM2 activator protein (GM2AP), and Ig-free light chain express differentially and may be used as lung cancer markers.[16]

As mentioned earlier, bodily fluids such as urine, sputum, blood, etc., could be used for biomarker detection. However, blood is currently the most commonly used fluid in lung cancer biomarker studies. It includes many biomarkers found in biopsied cancer tissues and many circulating protein fragments generated in the diseased tissue microenvironment or by circulating proteins derived from the diseased tissues.[3b,10]

Among various lung cancer biomarkers, CEA is one of the most extensively researched.[17] CEA is a large cell surface acidic glycoprotein with a molecular weight of about 200 kDa. The normal level of CEA in a healthy person ranges from 2.5 to 5 ng mL^{-1}, and its higher levels provide a useful prognostic indicator.[18] Other than CEA, NSE, a kind of neuroendocrine molecule, is a putative serum marker of SCLC and reveals high diagnostic sensitivity and specificity. A person having an NSE level higher than 35 ng mL^{-1} in serum is suspected of suffering from SCLC.[19] Further, ENO1 and Annexin II are other highly expressed biomarkers for lung cancer.[20]

Thus far, it has not been possible to identify a specific biomarker for lung cancer detection, and most biomarkers identified have been nonspecific indicators. Hence, a panel of biomarkers is generally studied for proper disease diagnosis.[6,8a,10,21] Patz et al. have shown that by using a protein biomarker panel of CEA, retinol binding protein (RBP), α1-antitrypsin (AAT), and squamous cell carcinoma (SCC) antigen, they were able to classify 88% of patients with lung cancer and 82% of patients without cancer correctly.[21a] It has also been shown that adding biomarkers like ENO1, SCC, NSE, CYFRA21-1, etc. to a panel containing CEA can improve sensitivity for lung cancer diagnosis.[6,21a]

Table 2 summarizes the DNA/genetic and protein-based biomarkers currently being investigated as markers for lung

Table 2. List of DNA/Genetic and Protein-Based Potential and Currently in Use Biomarkers in Lung Cancer Detection

group	biomarker
genetic biomarkers	RAR-β mRNA, COX2, DAPK, RASSFIA, IL-8 mRNA, PRCS3, FHIT, K-ras mutant, p53 mutant, epidermal growth factor receptor (EGFR) such as c-ErbB-1 and c-ErbB-2
protein biomarkers	CEA, CYFRA 21-1, TPA, tumor M2-pyruvate kinase, haptoglobin-α 2, APOA1, KLKB1, ProGRP, α-enolase (ENO1, also called neuron-specific enolase (NSE)), α-1-acid glycoprotein, chromogranin A, bombesin-like gastrin-releasing peptide, BB isoenzyme of creatine kinase (CK-BB), cytokeratin-7, carbohydrate antigen 19-9 (CA 19-9), carbohydrate antigen 125 (CA 125), plasma kallikrein B1, vascular endothelial growth factor (VEGF), cytokeratin fragment 21-1, nitrated ceruloplasmin, Annexin II, CD59 glycoprotein, transthyretin (TTR), GM2 activator protein (GM2AP), and Ig-free light chain

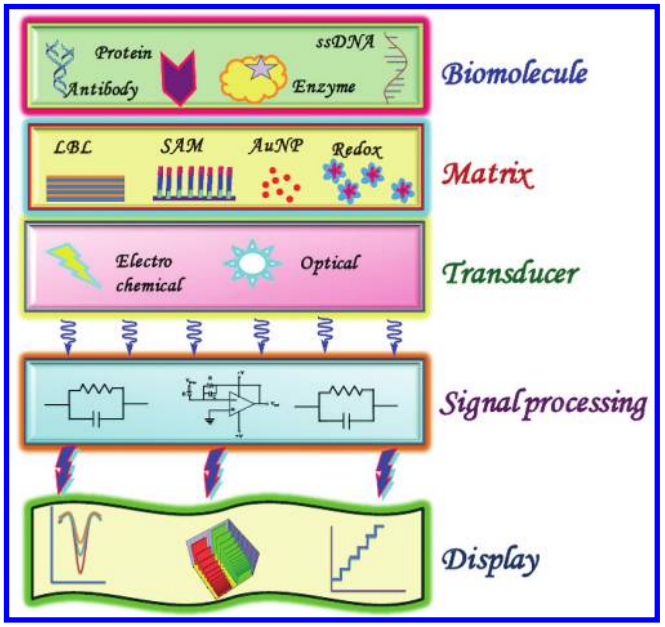

Figure 2. Schematic of biosensor.

cancer detection. Additional details on reliable biomarkers for prognosis and diagnosis of the disease can be found in the National Center for Biotechnology Information Web site and literature.[1b−d,2,3,10,16,20a,20b,21a,22]

1.4. Biomarker Detection for Early Stage Screening of Lung Cancer

In the early stages of the disease, only trace levels of biomarkers exist; hence, reliability and sensitivity of the screening tests is very crucial. As a rule of thumb, new detection technologies need to be at least 3 orders of magnitude better than the current state of the art for them to be seriously investigated for adoption. Biochemistry-, immunology-, and molecular biology-based methods and strategies are continuously being developed and used for increasingly sensitive determination of biomarkers in blood, urine, and other body fluids. Conventional approaches to biomarker detection are radio-immunoassay and enzyme-linked immunosorbent assay. These techniques are, however, complex, lab-based, slow, and require experienced personnel to conduct the analysis.[23] Further, optical immunoassay technique-based test methods have been proposed and are dominant in clinical quantitative detection of biomarkers. While these immunoassays are sensitive and selective, they are also time-consuming, expensive, multistep, and often require large and expensive equipment.[18b,20b,24] Additionally, some of these tests are not sufficiently sensitive for the detection of low level marker concentrations, which exist in the early stages of the disease.[1b,d] To address these challenges and for early screening of biomarkers, significant efforts are being invested by various research groups to develop biosensors for fast, accurate, and reliable detection of these early stage biomarkers. Biosensors have several potential advantages over other methods of detection, especially increased assay speed, flexibility, and simultaneous measurement of various analytes. The use of biosensors for protein biomarkers analysis has therefore been further highlighted as an attractive and cost-effective technique for the development of point-of-care devices. Figure 2 shows the schematic of biosensor assembly.

Among various biosensors, electrochemical biosensors have gained considerable interest as bioanalytical devices and have played an important role in the detection of cancer biomarkers at early stages.[25] They allow multitarget analyses, high sensitivity, lower detection limits, automation, reduced costs of testing, and development of disposable devices and methodologies capable of working with very small sample volumes.[21c,24f,26] Further, unlike spectroscopy-based techniques, electrochemical sensors are not affected by sample turbidity, quenching, or interference from absorbing and fluorescing compounds, and they require relatively simple instrumentation that is low-power and easily miniaturized.[21b] These biosensors measure the change in the electrochemical properties due to biomolecule−analyte interactions using voltammetric,[10−12] potentiometric,[27] amperometric,[21b,c] impedimetric,[20b,28] capacitive,[29] and conductometric[30] techniques. Among these, biosensors based on voltammetric techniques have received greater interest for reliable detection and analysis of lung cancer biomarkers, due to their simplicity and accuracy. In these biosensors, biorecognition molecules such as antibodies, aptamers, DNA, etc., are used for specific capture and sensitive detection of target analytes.

In early lung cancer analysis, various voltammetric techniques such as differential pulse voltammetry (DPV),[17a,d,g−j,21b,21d,31] cyclic voltammetry (CV),[17b,f,k,32] linear sweep voltammetry (LSV),[17l,22e] and square wave voltammetry (SWV)[17c,20a,33] have been reported to detect biomarkers. As can be seen in Table 3, use of electrochemical techniques, over optical and other transduction techniques, exhibits excellent sensitivity and a large linear detection range in a wide range of solvents, electrolytes, temperatures, etc. A significant contributor to this sensitivity is the matrix for immobilization of the capture biomolecules, which is discussed next.

2. MATRIX FOR RECOGNITION BIOMOLECULE IMMOBILIZATION

In the fabrication of a sensitive and reliable biosensor, the selection of a proper matrix for binding of recognition

Table 3. Characteristics of Various Biosensors for Lung Cancer Biomarker Detection

components	characteristics	reference
DPV-Based Biosensor		
[Mat]: colloidal Au/CHIT/SPCE	[L]: 0.5−25 ng mL^{-1}	17i
[CM]: CEA	[DL]: 0.22 ng mL^{-1}	
[Anal]: CEA	[S]: 0.95 nA (ng $mL^{-1})^{-1}$	
[MoI]: physical entrapment	[SL]: 25 days at 4 °C	
[DM]: thionine with H_2O_2	[CR]: 0.9981	
[IC]: CEA in 100 μL of diluted HRP-labeled anti-CEA, 35 °C, 20 min		
[MC]: 170 μL of 0.2 M PBS (pH 7.0) containing thionine (0.24 mM) and H_2O_2 (6.0 mM)		
[Tran]: DPV in −0.1 to −0.55 V (vs Ag/AgCl), with pulse amplitude (PA), 50 mV, pulse width (PW), 50 ms		
[Mat]: Thi/cellulose acetate/SPCE	[L]: CA 19-9, 0−24 U mL^{-1}	21d
[CM]: CA 19-9, CA 125	CA 125: 0−25 U mL^{-1}	
[Anal]: CA 19-9, CA 125	[DL]: CA 19-9, 0.2 U mL^{-1}	
[MoI]: physical coimmobilization	CA 125, 0.4 U mL^{-1}	
[DM]: H_2O_2	[SL]: 30 days at 4 °C	
[IC]: 50 μL of diluted HRP-labeled antibody and antigen, 1 h, room temp	[CR]: CA 19-9, 0.9992 CA 125, 0.9953	
[MC]: 4.5 mM H_2O_2 in 50 μL of PBS, pH 7.0		
[Tran]: DPV in 0.1 to −0.65 V (vs Ag/AgCl), with PA, 50 mV, PW, 50 ms		
[Mat]: biopolymer/sol−gel (APTES-TEOS-CHIT)/SPCE	[L]: (i) 0.4−140 kU L^{-1}	17j
[CM]: AuNP-HRP-labeled anti-(CA 153 or CA 125 or CA 199 or CEA)	(ii) 0.5−330 kU L^{-1}	
	(iii) 0.8−190 kU L^{-1}	
[BR]: 1% BSA in 0.1 M Tris-HCl (pH 7.2), 20 min	(iv) 0.1−44 μg L^{-1}	
[Anal]: (i) CA 153, (ii) CA 125, (iii) CA 199, and (iv) CEA	[DL]: (i) 0.2 kU L^{-1}	
[MoI]: physical entrapment	(ii) 0.5 kU L^{-1}	
[IC]: 20 μL of antigen, 40 min, room temp	(iii) 0.3 kU L^{-1}	
[MC]: 50 μL of 0.2 M PBS, pH 6.9	(iv) 0.1 μg L^{-1}	
[Tran]: DPV in −0.1 to −0.8 V (vs Ag/AgCl), with PA, 50 mV, PW, 50 ms	[S]: (i) 1.63 nA (kU $L^{-1})^{-1}$	
	(ii) 1.03 nA (kU $L^{-1})^{-1}$	
	(iii) 1.95 nA (kU $L^{-1})^{-1}$	
	(iv) 3.81 nA (μg $L^{-1})^{-1}$	
	[SL]: 35 day at room temp	
	[CR]: (i) 0.9916	
	(ii) 0.9959	
	(iii) 0.9936	
	(iv) 0.9930	
[Mat]: Thi/*p*-phthaloyl chloride/cysteamine/Au	[L]: 0.6−17 ng mL^{-1} and 17−200 ng mL^{-1}	17a
[CM]: anti-CEA loaded microtiter plate		
[Anal]: CEA	[DL]: 0.2 ng mL^{-1}	
[DM]: H_2O_2	[S]: 9.5 nA (ng $mL^{-1})^{-1}$ and 0.55 A (ng $mL^{-1})^{-1}$	
[IC]: 50 μL of CEA and 100 μL of HRP-labeled anti-CEA, 23 °C, 60 min		
[MC]: 2 mL of 0.2 mol L^{-1} H_2O_2 and 200 μL of eluted HRP-labeled anti-CEA	[SL]: 1 week at 4 °C	
	[Re]: three times	
[Tran]: DPV in 0.15 to −0.25 V (vs Ag/AgCl), with PA, 50 mV, PW, 60 ms, SR, 20 mV s^{-1}, pulse period 200 ms, sampling width 4 mV	[CR]: 0.9995 and 0.9880	
[Mat]: titania sol−gel/graphite electrode	[L]: 3−20 U mL^{-1}	31a
[CM]: CA 19-9	[DL]: 2.68 U mL^{-1}	
[Anal]: CA 19-9	[S]: 2.171 μA (U $mL^{-1})^{-1}$	
[MoI]: entrapment	[SL]: 3 weeks at 4 °C	
[DM]: catechol with H_2O_2	[CR]: 0.9965	

dx.doi.org/10.1021/cr100420s |*Chem. Rev.* 2011, 111, 6783–6809

Table 3. Continued

components	characteristics	reference
[IC]: 1.0 mL of HRP-anti CA 19-9 conjugate solution and 10 μL of CA 19-9 solution, 30 °C, 2 h [MC]: 0.1 mL of 5.0 mM catechol, 0.1 mL of 5.0 mM H_2O_2, and 0.8 mL of PBS [Tran]: DPV in 0.7 to −0.2 V (vs SCE), with PA, 50 mV, PW, 50 ms, 20 ± 0.5 °C [Mat]: ormosil sol−gel/graphite electrode [CM]: HRP-anti-CEA [Anal]: CEA [MoI]: physical entrapment	[L]: 0.5−3 ng mL^{-1} and 3−120 ng mL^{-1} [DL]: 0.4 ng mL^{-1} [S]: 1.12 μA (ng mL^{-1})$^{-1}$ and 0.088 μA (ng mL^{-1})$^{-1}$	17h
[IC]: 10 μL of CEA with 40 μL of enzyme conjugate, 30 °C, 35 min [MC]: 0.1 M PBS, pH 7.0 [Tran]: DPV in 0.2 to −0.2 V (vs SCE), with PA, 50 mV, PW, 50 ms	[SL]: 30 days at 4 °C [Re]: three times [CR]: 0.993 and 0.996	
[Mat]: AunNP-CHIT/ITO [CM]: CEA [BR]: BSA [Anal]: CEA [MoI]: physical adsorption [DM]: *o*-phenylenediamine (OPD) with H_2O_2 [IC]: 5 μL of CEA with 10 μL of a diluted HRP-labeled-anti-CEA, 35 °C, 20 min [MC]: 2 mM OPD and 0.5 mM H_2O_2 in 0.1 M PBS pH 5.0, 20 °C [Tran]: DPV in −0.3 to −0.8 V (vs Ag/AgCl), with PA, 50 mV, PW, 50 ms	[L]: 2−20 ng mL^{-1} [DL]: 1 ng mL^{-1} [SL]: 2 weeks at 4 °C [CR]: 0.997	17g
[Mat]: AuNPs/MWCNTs-CHIT/glassy carbon electrode (GCE) [CM]: anti-CEA [BR]: 0.25% BSA solution, 1 h [Anal]: CEA [MoI]: physical adsorption [IC]: CEA in 240 μL of 10 mM PBS, pH 6.0, 37 °C, 20 min [MC]: 10 mM PBS, pH 6.0 with 2.5 mM $[Fe(CN)_6]^{4-/3-}$ and 0.1 M KCl [Tran]: DPV	[L]: 0.3−2.5 ng mL^{-1} and 2.5−20 ng mL^{-1} [DL]: 0.01 ng mL^{-1} [S]: 4.0685 μA (ng mL^{-1})$^{-1}$ and 0.3693 μA (ng mL^{-1})$^{-1}$ [SL]: 30 days [Re]: six times [CR]: 0.981 and 0.993	17d 17e
[Mat]: AuNP/Au−Fe_3O_4 (core shell)/solid parafilm carbon paste electrode [CM]: anti-CEA [BR]: 1% BSA, 37 °C, 15 min [Anal]: CEA [MoI]: physical adsorption [DM]: hydroquinone with H_2O_2 [IC]: CEA in 1 mL of 20 mM PBS, pH 7.4 containing 25 μL of HRP-CEA and CEA, 37 °C, 20 min, 1000 rpm stirring [MC]: 1 mM hydroquinone and 2 mM H_2O_2 in 20 mM PBS, pH 7.4, 25 ± 0.5 °C [Tran]: DPV in 0.6 to −0.6 V (vs SCE), with PA, 50 mV, PW, 50 ms	[L]: 0.005−50 ng mL^{-1} [DL]: 0.001 ng mL^{-1} [S]: 2.575 μA (ng mL^{-1})$^{-1}$ [SL]: 40 days at 4 °C [CR]: 0.9988	
[Mat]: mercaptoundecanoic acid−phenylboronic acid conjugate/mercapto undecanol/Au	[L]: 2.5−40 ng mL^{-1}	31b

dx.doi.org/10.1021/cr100420s |*Chem. Rev.* 2011, 111, 6783–6809

Table 3. Continued

components	characteristics	reference
	[DL]: 1.1 ng mL^{-1}	
[CM]: HRP-anti-CEA	[CR]: 0.9929	
[Anal]: CEA		
[MoI]: physical adsorption		
[DM]: Thi with H_2O_2		
[IC]: CEA, 35 °C, 60 min		
[MC]: 6 mM H_2O_2 and 20 μM thionine in 5 mL of 0.1 M PBS, pH 8.5, 25 ± 2 °C		
[Tran]: DPV in 0.0 to −0.4 V (vs SCE)		
[Mat]: APTES/$CoFe_2O_4$/CPE/magnet (0.3 T)	[L]: 1.5−60 ng mL^{-1}	40
[CM]: HRP-anti-CEA	[DL]: 0.5 ng mL^{-1}	
[BR]: HRP, 1 mg mL^{-1} in PBS, 37 °C, 1 h	[S]: 2.44 nA (ng $mL^{-1})^{-1}$	
[Anal]: CEA	[SL]: 17 days at 4 °C	
[MoI]: covalent via glutaraldehyde	[CR]: 0.985	
[DM]: H_2O_2		
[IC]: 1.5 mL of CEA solution, 40 min, room temp		
[MC]: 1.5 mL of 0.1 PBS, pH 6.8 with 0.35 mM H_2O_2 at rate of 1.5 mL min^{-1}, room temp (25 ± 0.5 °C)		
[Tran]: DPV in 0−0.4 V (vs Ag/AgCl), with PA, 50 mV, PW, 50 ms		
CV-Based Biosensor		
[Mat]: AuNP/L-cystein/Nafion/Au	[L]: 0.01−100 ng mL^{-1}	17f
[CM]: anti-CEA	[DL]: 3.3 pg mL^{-1}	
[BR]: BSA	[S]: 4.46 μA (ng $mL^{-1})^{-1}$	
[Anal]: CEA	[CR]: 0.9960	
[MoI]: physical adsorption		
[IC]: CEA incubation for 12 min, 30 °C		
[MC]: 5 mM $[Fe(CN)_6]^{4-/3-}$ solution containing 0.1 M KCl, pH: 7.0		
[Tran]: CV in −0.2 to 0.6 V (vs SCE), SR: 50 mV s^{-1}		
[Mat]: AuNPs/PTC-NH_2/PB/GCE	[L]: 0.05−2 ng mL^{-1} and 2−40 ng mL^{-1}	32a
[CM]: anti-CEA		
[BR]: 0.25% BSA solution, 1 h, 25 °C	[DL]: 0.018 ng mL^{-1}	
[Anal]: CEA	[S]: 11.801 μA (ng $mL^{-1})^{-1}$ and	
[MoI]: physical adsorption	1.4248 μA (ng $mL^{-1})^{-1}$	
[IC]: CEA in 1 mL of 25 mM PBS, pH 6.0, 25 °C, 20 min	[SL]: 60 days at 4 °C	
[MC]: 5 mL of 25 mM PBS, pH 6.0, room temp	[CR]: 0.996 and 0.995	
[Tran]: CV in −0.2 to 0.5 V (vs SCE), SR: 50 mV s^{-1}		
[Mat]: protein A/nano-Au/$Co(bpy)_3^{3+}$/BSA−HRP membrane/Au	[L]: 0.5−80 ng mL^{-1}	32b
[CM]: anti-CEA	[DL]: 0.14 ng mL^{-1}	
[BR]: HRP	[S]: 0.2858 μA (ng $mL^{-1})^{-1}$	
[Anal]: CEA	[SL]: 30 days at 4 °C	
[MoI]: physical adsorption	[Re]: six times	
[DM]: H_2O_2	[CR]: 0.9973	
[IC]: CEA solution at room temp, 10 min		
[MC]: 2 mM H_2O_2 in 5 mL of 0.01 M PBS, pH 7, room temp		
[Tran]: CV in −0.4 to 0.5 V (vs SCE), SR: 50 mV s^{-1}		
[Mat]: AuNPs/CHIT/nano gold/GCE	[L]: 0.2−120 ng mL^{-1}	17b
[CM]: anti-CEA	[DL]: 0.06 ng mL^{-1}	
[BR]: 0.25% BSA solution, 1 h, 35 °C	[S]: 1310 nA (ng $mL^{-1})^{-1}$	
[Anal]: CEA	[SL]: 90 days at 4 °C	
[MoI]: physical adsorption	[Re]: eight times	
[IC]: CEA in 10 mM PBS, pH 7.0, 35 °C, 20 min	[CR]: 0.9981	

Table 3. Continued

components	characteristics	reference
[MC]: 5 mM $[Fe(CN)_6]^{4-/3-}$ solution containing 0.1 M KCl, pH: 7.0, 35 °C		
[Tran]: CV in −0.2 to 0.6 V (vs SCE), SR: 50 mV s^{-1}		
[Mat]: Au/BSA/[Ag−Ag_2O]/SiO_2 nanocomposite/GCE	[L]: 0.5−160 ng mL^{-1}	17k
[CM]: anti-CEA	[DL]: 0.14 ng mL^{-1}	
[BR]: 0.25% BSA solution, 20 min, room temp	[S]: 4.0685 μA (ng $mL^{-1})^{-1}$	
[Anal]: CEA	[SL]: 10 days at 4 °C	
[MoI]: physical adsorption	[CR]: 0.9924	
[IC]: CEA in 0.1 M HAc−NaAc buffer, pH 5.5, 7 min, room temp		
[Tran]: CV in −0.6 to 0.6 V (vs SCE), SR: 100 mV s^{-1}		
[Mat]: $(AuNP/thionine\ (Thi^+))_n$/nano-Au/nano-$TiO_2$/Au	[L]: 0.2−80 ng mL^{-1}	32c
[CM]: anti-CEA	[DL]: 0.07 ng mL^{-1}	
[BR]: HRP (1 mg mL^{-1}), 4 °C, 1 h	[S]: 60 days	
[Anal]: CEA		
[MoI]: physical adsorption		
[DM]: H_2O_2		
[IC]: CEA in HAc−NaAc buffer, pH 6.0, 25 °C, 15 min		
[MC]: 0.55 mM H_2O_2 in HAc−NaAc buffer, pH 6.0, room temp		
[Tran]: CV in −0.4 to 0.1 V (vs SCE), SR: 50 mV s^{-1}		
[Mat]: APTMS/SiO_2/Si	[DL]: 1 fg mL^{-1} for IL-10 and 1 pg mL^{-1} for OPN	32d
[CM]: anti-IL10 and anti-OPN		
[BR]: protein array blocking solution, 2 h, room temp		
[Anal]: IL10 and OPN		
[MoI]: physical adsorption		
[DM]: *p*-NPP		
[IC]: (i) antigen incubation, 2 h, room temp, (ii) 2 h incubation with a biotinylated detector antibody, and (iii) 30 min of incubation with a streptavidin-coated alkaline phosphatase enzyme		
[MC]: 30 μL of *p*-NPP, 20 min, room temp		
[Tran]: CV (vs Ag) in 0.5−1.1 V, SR: 50 mV s^{-1}		
[Mat]: thioctic acid-AuNW/Au (interdigitated array; IDA)	[L]: 10−100 ng mL^{-1}	22d
[CM]: anti-CK	[DL]: 10 ng mL^{-1}	
[BR]: BSA, 1 h	[CR]: 0.996	
[Anal]: cytokeratin-7		
[MoI]: physical adsorption		
[DM]: *p*-nitrophenyl phosphate		
[IC]: (i) cytokeratin-7, 1 h, (ii) biotinilated anti-CK7, 1 h, (iii) streptavidin−alkaline phosphatase (AP) enzyme (100 μL), 30 min		
[MC]: 30 μL of *p*-NPP, 20 min, room temp		
[Tran]: CV in −0.2 to 0.25 V (vs Ag/AgCl), SR: 100 mV s^{-1}		
[Mat]: poly(sodium-*p*-styrenesulfonate)/AuNPs-MWNTs-Thi-CHIT/MPS/Au	[L]: 0.5−15 and 15−200 ng mL^{-1} [DL]: 0.01 ng mL^{-1}	35d
[CM]: anti-CEA	[S]: 3.87 and 0.48 μA (ng $mL^{-1})^{-1}$	
[BR]: BSA, 1 h, 4 °C	[SL]: 60 days at 4 °C	
[Anal]: CEA	[Re]: 10 times	
[MoI]: physical adsorption	[CR]: 0.9968 and 0.9966	
[IC]: CEA solution, 25 °C, 10 min		
[MC]: 5 mL of 0.1 M PBS, pH 6.5, 25 ° C		
[Tran]: CV in −0.6 to 0.2 V (vs SCE), SR: 50 mV s^{-1}		
[Regen]: 5 M urea, 5 min		
[Mat]: AuNP/poly(toluidine blue O) /DNA−PDDA/GC	[L]: 0.5−120 ng mL^{-1}	35b
[CM]: anti-CEA	[DL]: 0.3 ng mL^{-1}	

Table 3. Continued

components	characteristics	reference
[BR]: 0.25% BSA, 1 h, room temp	[S]: 0.106 μA (ng mL^{-1})$^{-1}$	
[Anal]: CEA	[SL]: 30 days at 4 °C	
[MoI]: physical adsorption	[Re]: five times	
[IC]: CEA solution, 25 °C, 10 min	[CR]: 0.997	
[MC]: 5 mL of 0.1 M PBS, pH 6.5, 25 °C		
[Tran]: CV in −0.6 to 0.2 V (vs SCE), SR: 50 mV s^{-1}		
[Mat]: AuNP/nano-$CaCO_3$/PB/GC	[L]: 0.3−20 and 20−100 ng mL^{-1}	41
[CM]: anti-CEA	[DL]: 0.1 ng mL^{-1}	
[BR]: 0.25% BSA, 2 h	[S]: 1.87 and 0.35 μA (ng mL^{-1})$^{-1}$	
[Anal]: CEA	[SL]: 2 weeks at 4 °C	
[MoI]: physical adsorption	[Re]: five times	
[IC]: CEA solution in PBS pH 6.5, 12 min	[CR]: 0.9916 and 0.995	
[MC]: 0.025 M PBS, pH 6.5, 25 °C		
[Tran]: CV in −0.2 to 0.5 V (vs SCE), SR: 50 mV s^{-1}		
[Regen]: 5 M urea, 5 min		
[Mat]: AuNP/Thi/GA/porous CHIT/GC	[L]: 0.2−10 and 10−160 ng mL^{-1}	24f
[CM]: anti-CEA	[DL]: 0.08 ng mL^{-1}	
[BR]: 0.25% BSA, 1 h, 25 °C	[S]: 1.2 and 0.1 μA (ng mL^{-1})$^{-1}$	
[Anal]: CEA	[SL]: 45 days at 4 °C	
[MoI]: physical adsorption	[CR]: 0.997 and 0.998	
[IC]: CEA solution, 25 °C, 10 min		
[MC]: 0.1 M HAc−NaAc buffer, pH 5.5		
[Tran]: CV in −0.6 to 0.2 V (vs SCE), SR: 50 mV s^{-1}		
[Mat]: AuNPs/PBNPs/AuNPs−MWNTs−CHIT/GCE	[L]: 0.3−120 ng mL^{-1}	42
[CM]: anti-CEA	[DL]: 0.1 ng mL^{-1}	
[BR]: 0.25% BSA, 1 h	[S]: 0.6886 ± 0.0119 μA (ng mL^{-1})$^{-1}$	
[Anal]: CEA	[SL]: 30 days at 4 °C	
[MoI]: physical adsorption	[CR]: 0.9976	
[IC]: CEA solution in 0.025 M PBS pH 6, 12 min, room temp		
[MC]: 0.025 M PBS pH 6		
[Tran]: CV in −0.4 to 0.8 V (vs SCE), SR: 50 mV s^{-1}		
[Regen]: 4 M urea, 5 min		
[Mat]: AuNPs/TB/PSAA/GCE	[L]: 0.5−5 and 5−120 ng mL^{-1}	26
[CM]: anti-CEA	[DL]: 0.2 ng mL^{-1}	
[BR]: HRP 1 mg mL^{-1}, 2 h, 4 °C	[SL]: 20 days at 4 °C	
[Anal]: CEA	[Re]: eight times	
[MoI]: physical adsorption		
[DM]: H_2O_2		
[IC]: CEA solution in 0.1 M PBS pH 7.4, 10 min, 30 °C		
[MC]: 1 mL of 0.1 PBS, 0.1 M KCl, pH 6.5 with 0.3 mM H_2O_2		
[Tran]: CV in −0.6 to 0.1 V (vs SCE), SR: 50 mV s^{-1}, 25 °C		
[Regen]: 0.04 M HCl, 5 min		
[Mat]: protein A/AuNPs/CFME	[L]: 0.01−160 ng mL^{-1}	34
[CM]: anti-CEA	[DL]: 5 pg mL^{-1}	
[Anal]: CEA	[S]: 0.758 μA (ng mL^{-1})$^{-1}$	
[MoI]: physical adsorption	[SL]: 19 days at 4 °C	
[DM]: H_2O_2	[CR]: 0.982	
[IC]: (i) CEA solution, 20 min, room temp, (ii) Thi doped magnetic gold nanospheres labeled HRP-anti-CEA, 20 min, room temp		
[MC]: acetic acid buffer, pH 6.8, 0.75 mM H_2O_2		
[Tran]: CV vs SCE		
[Regen]: 0.1 M glycine−HCl, pH 2, 5 min		
[Mat]: $(AuNPs/Thi)_4$/Nafion/Au	[L]: 2.5−80 ng mL^{-1}	35c

dx.doi.org/10.1021/cr100420s |*Chem. Rev.* 2011, 111, 6783–6809

Table 3. Continued

components	characteristics	reference
[CM]: anti-CEA	[DL]: 0.9 ng mL^{-1}	
[BR]: HRP 0.25%, 2 h, pH 6.5	[S]: 0.0863 μA (ng mL^{-1})$^{-1}$	
[Anal]: CEA	[SL]: 45 days at 4 °C	
[MoI]: physical adsorption	[Re]: six times	
[DM]: H_2O_2	[CR]: 0.9972	
[IC]: CEA solution, 10 min, 25 ± 0.5 °C		
[MC]: 5 mL of 0.1 M HAc−NaAc buffer, pH 5.5, 0.31 mM H_2O_2, 25 °C		
[Tran]: CV in −0.6 to 0.2 V (vs SCE), SR: 50 mV s^{-1}		
[Regen]: 4 M urea		
[Mat]: AuNPs/SiO_2−Thi nanocomposite/AuNPs/Cys/Au	[L]: 1−100 ng mL^{-1}	36b
[CM]: anti-CEA	[DL]: 0.34 ng mL^{-1}	
[BR]: BSA, 2 h, 4 °C	[S]: 0.7314 μA (ng mL^{-1})$^{-1}$	
[Anal]: CEA	[SL]: 30 days at 4 °C	
[MoI]: physical adsorption	[Re]: seven times	
[IC]: CEA solution in HAc−NaAc buffer, 10 min, 37 °C	[CR]: 0.9922	
[MC]: 5 mL of 0.1 M HAc−NaAc buffer, pH 5.5		
[Tran]: CV in −0.6 to 0.2 V (vs SCE), SR: 50 mV s^{-1}		
[Regen]: 4 M urea		
[Mat]: CHIT−AuNPs/APTES/PB−SiO_2/GCE	[L]: 0.25−5 and 7−75 ng mL^{-1}	19b
[CM]: anti-NSE	[DL]: 0.08 ng mL^{-1}	
[BR]: 1% BSA, 2 h, 4 °C	[S]: 2.55 and 0.603 μA (ng mL^{-1})$^{-1}$	
[Anal]: NSE	[SL]: 20 days at 4 °C	
[MoI]: physical adsorption	[CR]: 0.9899 and 0.9894	
[DM]: H_2O_2		
[IC]: NSE solution, 35 min, 37 °C		
[MC]: 5 mL of 0.1 M PBS, pH 7, 0.75 mM H_2O_2		
[Tran]: CV in −0.6 to 0.2 V (vs SCE), SR: 50 mV s^{-1}		
LSV- and SWV-Based Biosensor		
[Mat]: jeffamine/carbon fiber micro electrode (CFME)	[L]: 38−100 pg mL^{-1}	22e
[CM]: ferrocene monocarboxylic acid-anti-VEGF	[DL]: 38 pg mL^{-1}	
[Anal]: VEGF	[SL]: 24 days at 4 °C	
[MoI]: covalent (cross-linking)		
[IC]: VEGF in 1 mL of 0.15 M NaCl, room temp, 40 min		
[MC]: 0.5 M $NaClO_4$		
[Tran]: LSV in 0 to 0.7 V (vs Ag/AgCl), SR: 0.75 V s^{-1}		
[Mat]: MWCNT-polyethyleneimine/SPE	[L]: 5×10^{-12}−5×10^{-7} g mL^{-1}	33
[CM]: anti-CEA	[DL]: 1×10^{-12} g mL^{-1}	
[BR]: ethanolamine and 0.1% BSA in PBS (0.1 M, pH 7.0)		
[Anal]: CEA		
[MoI]: covalent via glutaraldehyde		
[DM]: ferrocene carboxylic acid encapsulated liposomes (FCL)		
[IC]: (i) 50 μL of the CEA solution, 30 min, 25 ± 3 °C, (ii) anti-CEA-FCL (10 μL in 100 μL of PBS (0.01 M, pH 7.0)), 25 ± 3 °C, 30 min		
[MC]: eluted FCL in 100 μL of methanolic solution of Triton X (2%) in PBS (0.1 M, pH 7.0)		
[Tran]: SWV (vs Ag/AgCl) in −0.3 to 0.5 V, potential steps, 4 mV; frequency, 25 Hz; and amplitude, 50 mV		
[Mat]: carbon nanoparticles/poly(ethylene imine)/SPGE	[L]: 0.032−10 ng mL^{-1}	17c
[CM]: anti-CEA	[DL]: 32 pg mL^{-1}	

Table 3. Continued

components	characteristics	reference
[Anal]: CEA [MoI]: covalent via glutaraldehyde [DM]: cadmium sulphide nanocrystal quantum dots (CdS QDs) [IC]: (i) CEA in 5 μL of Tris-HCl buffer, 20 min, (ii) 15 min with anti-CEA-CdS QDs in 5 μL of the Tris-HCl buffer [MC]: CdS QD elution in HNO_3 (0.1 M, 5 μL) and an acetate buffer (0.1 M, pH 4.6, 40 μL) spiked with mercury(II) nitrate (65 ppm) [Tran]: SWV (vs Ag/AgCl) in −1.0 to −0.1 V potential steps, 4 mV; frequency, 15 Hz; amplitude, 25 mV		
[Mat]: polyethylene glycol/SPCE [CM]: anti-ENO1 [BR]: 5 μL of 0.1% casein, 20 min [Anal]: ENO1 [MoI]: physical adsorption [DM]: AuNPs [IC]: (i) 5 μL of ENO1, 1 h, (ii) 5 μL of AuNP-anti-ENO1, 40 min [MC]: (i) AuNP oxidation in 0.1 M HCl at 1.2 V, 120 s, (ii) Au reduction to Au^0 at 0.35 V [Tran]: SWV in 0.8 to 0 V (vs Ag), potential steps, 4 mV; frequency, 15 Hz; amplitude, 25 mV	[L]: 10^{-12}−10^{-8} g mL^{-1} [DL]: 11.9 fg [limit of quantification]: 103 fg	20a
[Mat]: SPCE [CM]: anti CEA on carboxyl modified magnetic beads [BR]: for magnetic beads, 500 μL of 30 mM glycine, 30 min; after immune assay, 200 μL of 1% BSA in PBS, 30 min [Anal]: CEA [MoI]: covalent via EDC/NHS [DM]: Hg [IC]: (i) 5 μL of CEA, 1 h, (ii) 10 μL of PbS NPs with 40 μL of PBS, 1 h [MC]: (i) lead component release in 10 μL of 1 M HCl, 180 s, (ii) lead suspension with 90 μL of 0.2 M acetate buffer containing 20 μg mL^{-1} Hg, (iii) 100 μL of mix on SPCE [Tran]: (i) 65 s pretreatment at 0.6 V, (ii) 120 s accumulation at −1.4 V, (iii) SWV after a 5 s rest period from −1.0 to −0.4 V (vs Ag/AgCl); step potential, 4 mV; amplitude, 25 mV; frequency, 15 Hz	[L]: 1−50 ng mL^{-1} [DL]: 0.5 ng mL^{-1}	23c
Amperometric and Other Electrochemical Techniques-Based Biosensor		
[Mat]: IrO_2/glass [CM]: AFP, ferritin, CEA, hCG-β, CA 15-3, CA 125, and CA 19-9 [BR]: seablock, 20 min [Anal]: AFP, ferritin, CEA, hCG-β, CA 15-3, CA 125, and CA 19-9 [MoI]: physical adsorption [DM]: hydroquinone diphosphate [IC]: (i) 500 μL of antigen and antibody mixture in blocking buffer, 2 h (ii) 5 μg mL^{-1} AP-anti-GIgG and 7.5 μg mL^{-1} AP-anti-MIgG in 600 μL of blocking buffer, 2 h [MC]: 1 mL of 100 mM Tris-HCl, 200 mM KCl, 10 mM $MgCl_2$, pH 9.0,	[DL]: 1.4 (AFP), 7.0 (ferritin) (CEA), and 1.8 ng mL^{-1} (hCG-β), 1.2 and 0.7 (CA 15-3), 1.2 (CA 125), and 1.0 U mL^{-1} (CA 19-9) [S]: 0.967 (AFP); 1.012 (ferritin); 0.964 (CEA); 1.086 (hCG-β); 1.008 (CA 15-3); 1.062 (CA 125); and 1.006 (CA 19-9) [CR]: 0.9981 (AFP); 0.9985 (ferritin); 0.9978 (CEA); 0.9906 (hCG-β); 0.9991 (CA 15-3); 0.9921 (CA 125); and 0.9981 (CA)	21c

Table 3. Continued

components	characteristics	reference
2 mM hydroquinone diphosphate		
[Tran]: amperometric (vs Ag/AgCl), 320 mV		
[Mat]: APTES/IrO_2/glass	[L]: CEA, 25−150 ng mL^{-1}; AFP, 10−200 ng mL^{-1}	21b
[CM]: anti-CEA and anti-AFP		
[BR]: 1% BSA in 0.1 M tris-HCl, pH 7.2, 60 min	[DL]: CEA, 1.2 ng mL^{-1}; AFP, 1 ng mL^{-1}	
[Anal]: CEA and AFP		
[MoI]: covalent via glutaraldehyde		
[DM]: hydroquinone diphosphate		
[IC]: (i) CEA/AFP in 200 μL of blocking buffer, 60 min, (ii) 1 μg mL^{-1} biotin-anti- CEA/AFP in 200 μL of blocking buffer, 60 min, (iii) 0.5 μg mL^{-1} streptavidin-labeled AP in 200 μL of blocking buffer, 60 min		
[MC]: 1 mL of 100 mM Tris-HCl, 200 mM KCl, 10 mM $MgCl_2$, pH 9.0, 1 mM hydroquinone diphosphate		
[Tran]: amperometric (vs Ag/AgCl), 420 mV		
[Mat]: AuNPs/GCE	[L]: 2−80 ng mL^{-1}	18c
[CM]: anti-CEA	[DL]: 0.6 ng mL^{-1}	
[BR]: 10 mg mL^{-1} BSA, 1 h, 37 °C		
[Anal]: CEA		
[MoI]: physical adsorption		
[MC]: 0.1 M PBS, pH 7, containing 2.5 mM $Fe(CN)_6^{3-/4-}$		
[Tran]: EIS in 50−10^6 Hz at bias potential: 0.17 V, AC amplitude 10 mV		
[Mat]: hydrazine sulfate/AuNPs/dendrimer/poly-TTCA/AuNPs/GCE	[L]: 0−0.15 μg mL^{-1}	20b
	[S]: 3140 ± 231.93 Ω (μg mL^{-1})$^{-1}$	
[CM]: anti-Annexin II	[CR]: 0.994	
[Anal]: Annexin II		
[MoI]: covalent via glutaraldehyde		
[MC]: 0.1 M PBS, pH 7, containing 4 mM $Fe(CN)_6^{3-/4-}$/0.3 M $NaClO_4$		
[Tran]: EIS (vs Ag/AgCl) at OCP in 0.1−10^5 Hz at, AC amplitude 10 mV		
[Mat]: GPMS/$(Fe_3O_4)_{core}$−$(SiO_2)_{shell}$/CPE via external magnet	[L]: 1.5−60 ng mL^{-1}	43
[CM]: anti-CEA	[DL]: 0.5 ng mL^{-1}	
[BR]: 1.5 mL of 1% BSA, 12 h	[S]: 34.8 Ω (ng mL^{-1})$^{-1}$	
[Anal]: CEA	[SL]: 2 weeks	
[MoI]: covalent via epoxide coupling	[CR]: 0.992	
[IC]: CEA solution, 30 min		
[MC]: PBS, pH 7.4, containing 10 mM $Fe(CN)_6^{3-/4-}$		
[Tran]: EIS (vs Ag/AgCl) in 10^{-2}−10^6 Hz at bias potential: 0.17 V, AC amplitude 50 mV		
[Regen]: magnet removal		
[Mat]: poly *o*-aminophenol/Au	[L]: 0.5−20 ng mL^{-1}	28
[CM]: anti-CEA covalently attached to glutathione modified AuNP	[DL]: 0.1 ng mL^{-1}	
[Anal]: CEA	[S]: 1.079 × 10^5 Ω (ng mL^{-1})$^{-1}$	
[MoI]: electro-copolymerization	[CR]: 0.9821	
[IC]: 200 μL of CEA solution, 40 min		
[MC]: PBS (1/15 M pH 7.4) containing 5 mM $Fe(CN)_6^{3-/4-}$		
[Tran]: EIS (vs SCE) in 0.1−10^5 Hz at OCP, AC amplitude 5 mV		
[Mat]: thiourea/Au	[L]: 0.01−10 ng mL^{-1}	29a
[CM]: anti-CEA	[DL]: 10 pg mL^{-1}	
[BR]: 0.1 M ethanol amine, pH 8.0, 30 min	[S]: 31 nF cm^{-2} (ng mL^{-1})$^{-1}$	

Table 3. Continued

components	characteristics	reference
[Anal]: CEA	[SL]: 3 days	
[MoI]: covalent via glutaraldehyde	[Re]: 45 times	
[IC]: CEA in 10 mM Tris-HCl, pH 7.0	[CR]: 0.999	
[Tran]: capacitance (vs Ag/AgCl), potential step: 50 mV		
[Regen]: HCl, pH 2.0		
Optical Techniques-Based Biosensor		
[Mat]: DNA/11-amino-1-undecanethiol/Au	[DL]: 1 pM	45
[CM]: ssRNA aptamer		
[Anal]: VEGF protein		
[MoI]: RNA−DNA ligation using T4 RNA ligase enzyme		
[DM]: 3,3′,5,5′-tetramethylbenzidine		
[IC]: (i) 1 pM VEGF solution 15 min, (ii) 10 nM VEGF antibody 10 min, (iii) antibiotin HRP solution (50 nM) 10 min, (iv) TMB solution		
[Tran]: SPR imaging		
[Mat]: biotinylated protein A/neutravidine/Au	[DL]: 30 ng mL^{-1}	46
[CM]: anti-CEA		
[BR]: 10 mg mL^{-1} BSA solution, 30 min		
[Anal]: CEA		
[MoI]: biotin−neutravidin binding		
[IC]: 35 μL of CEA, 30 min, 37 °C		
[Tran]: SPR		
[Mat]: immunoaffinity column	[L]: 1−25 ng mL^{-1}	18b
[CM]: CEA	[DL]: 0.5 ng mL^{-1}	
[BR]: 0.1 mol L^{-1} $NaHCO_3$/0.2 mol L^{-1} glycine, pH 8.5, 24 h, 4 °C	[Re]: 30 times	
[Anal]: CEA	[CR]: 0.997	
[MoI]: physical adsorption		
[DM]: luminol, PIP, and H_2O_2 mixture		
[IC]: 50 μL of diluted HRP-labeled anti-CEA solution in 0.1 mol/L pH 7.0 PBS and 50 μL of CEA standard solution, at a flow rate of 0.1 mL min^{-1}		
[MC]: 100 μL mixture of 0.1 mol L^{-1} pH 8.5 Tris−HCl buffer solution containing 1.0 mmol L^{-1} H_2O_2, 0.5 mmol L^{-1} luminol, and 0.4 mmol L^{-1} PIP		
[Tran]: chemiluminescence		
[Regen]: 0.1 mol L^{-1} pH 2.2 glycine−HCl		
[Mat]: ultrabind aldehyde active membrane	[L]: CEA, 1−120 ng mL^{-1}; CA125, 5−100 U mL^{-1}	24a
[CM]: anti-CEA and anti-CA125		
[BR]: PBS containing 0.5% BSA and 0.5% casein	[DL], 0.6 ng mL^{-1}; CA125, 1.5 U mL^{-1}	
[Anal]: CEA and CA-125		
[MoI]: covalent via aldehyde groups	[SL]: 10 days at 4 °C	
[DM]: for CA-125, HRP substrate based on the luminol-PIP-H_2O_2	[Re]: 20 times	
for CEA: ALP substrate based on the disodium 3-(4-methoxyspiro-(1,2-dioxetane-3,2′-(5′-chloro) tricycle[3.3.1.13,7] decan)-4-yl) phenyl phosphate	[CR]: 0.9995 (CEA), 0.9954 (CA-125)	
[IC]: 25 μL of CEA/CA-125 with enzyme labeled CA 125, and CEA antibodies, room temperature, 20 min		
[MC]: HRP and ALP substrate, 4 min		
[Tran]: chemiluminescence		
[Regen]: 0.1 M glycine−HCl, pH 2.0		
[Mat]: aldehyde activated polyethersulfone membrane	[L]: CEA, 1−70 ng mL^{-1}	44
[CM]: anti-CEA and anti-CA 19-9	CA 19-9, 5−150 U mL^{-1}	

dx.doi.org/10.1021/cr100420s |*Chem. Rev.* 2011, 111, 6783–6809

Table 3. Continued

components	characteristics	reference
[BR]: PBS containing 0.5% BSA and 0.5% casein	[DL]: 0.65 ng mL^{-1}	
[Anal]: CEA and CA-199	CA 19-9: 2 U mL^{-1}	
[MoI]: covalent via aldehyde groups	[S]: CEA, 5.6; CA 19-9, 11.0	
[DM]: for CEA, HRP substrate based on the luminol-PIP-H_2O_2	[SL]: 20 days at 4 °C	
for CA 19-9, ALP substrate based on the disodium 3-(4-methoxyspiro-(1,2-dioxetane-3,2′-(5′-chloro) tricycle[3.3.1.13,7] decan)-4-yl) phenyl phosphate	[Re]: 20 times	
[IC]: CEA/CA-199 with enzyme labeled CA 199 and CEA antibodies, room temperature, 20 min	[CR]: 0.995 (CEA), 0.995 (CA 19-9)	
[MC]: HRP and ALP substrate, 4 min		
[Tran]: chemiluminescence		
[Regen]: 0.1 M glycine−HCl, pH 2.0		
[Mat]: 96-well microtiter plate	[DL]: CEA, 0.3 ng mL^{-1}	24c
[CM]: anti-CEA and anti-AFP	AFP: 0.07 ng mL^{-1}	
[Anal]: CEA and AFP		
[MoI]: physical adsorption		
[DM]: AFP, BHHCT-Eu^{3+}; CEA, BHHCT-Sm^{3+}		
[IC]: (i) 50 μL of AFP−CEA solution, 37 °C, 1 h; (ii) 50 μL mixture of BHHCT-Eu^{3+}-labeled anti-AFP and biotinylated anti-CEA 37 °C, 1 h; (iii) 50 μL of the $SA(BSA)_{0.9}(BHHCT)_{46}$−$Sm^{3+}$ solution, 37 °C, 1 h; (iv) 50 μL of 0.1 M NaOH containing 1.0×10^{-5} M TOPO and 0.05% SDS, room temperature, 10 min		
[MC]: (i) solid phase Eu time-resolved fluorometric measurement with excitation at 340 nm, emission at 615 nm with delay time of 0.2 ms and window time of 0.4 ms, (ii) solution phase Sm time-resolved fluorometric measurement with excitation at 340 nm, emission at 643 nm with delay time of 0.03 ms, and window time of 0.1 ms		
[Tran]: time-resolved fluoroimmunoassay		
[Mat]: immunoaffinity column having sepharose gel	[L]: 2.5−100 ng mL^{-1}	24d
[CM]: anti-CEA	[DL]: 1 ng mL^{-1}	
[BR]: 1% BSA in PBS (pH 7.0), 24 h, °C	[Re]: 15 times	
[Anal]: CEA	[CR]: 0.997	
[MoI]: physical entrapment		
[DM]: europium		
[IC]: (i) 100 μL of CEA solution in 0.1 M pH 7.0 PBS, 10 min, (ii) 100 μL of diluted Eu-labeled anti-CEA solution, 10 min, room temperature (25 ± 2 °C), (iii) 300 μL of the enhancement solution to cleave the Eu-labels at a flow rate of 0.1 mL min^{-1}		
[MC]: 300 μL of the outflow solution and 280 μL of effluent		
[Tran]: time-resolved fluorometry		
[Regen]: 0.1 M glycine−HCl (pH 2.2), 1 min		
[Mat]: nitrocellulose membrane	[L]: 10 μg mL^{-1}−1 ng mL^{-1}	22f
[CM]: anticeruloplasmin	[DL]: 0.4 ng mL^{-1}	
[BR]: 1% casein, room temp, 30 min	[SL]: 3 months at 4 °C	
[Anal]: nitrated ceruloplasmin		
[MoI]: physical adsorption		
[DM]: Qdot 585 modified antinitrotyrosine		
[MC]: lateral flow for 10 min		
[Tran]: fluorescence		
[Mat]: magnetic nanoparticles	[L]: 1−10 pg mL^{-1}	47
[CM]: anti-CEA	[DL]: 1 pg mL^{-1}	
[BR]: 3 mM ethanolamine, 2 h		
[Anal]: CEA		

Table 3. Continued

components	characteristics	reference
[MoI]: covalent via EDC/NHS [DM]: anti-CEA modified hollow gold nanospheres HGNs with 4,4′-dipyridyl (DP) [IC]: (i) 10 μL of 0.5 mg mL^{-1} anti-CEA-magnetic beads with 10 μL of PBS containing 50 ng mL^{-1} of CEA antigen, 20 min, (ii) 10 μL of 0.7 nM anti-CEA-HGNs, 20 min [MC]: immunocomplex molecules in capillary tube [Tran]: SERS in 900−1800 cm^{-1} with 632.8 nm laser of 30 mW		
Other Techniques-Based Biosensor		
[Mat]: AuNP/hydroxylamine/MPTS/Au (QCM) [CM]:anti-CEA [BR]: 10 mg mL^{-1} BSA in PBS, 1 h, 37 °C [Anal]: CEA [MoI]: physical adsorption [IC]: CEA sample, pH 7.0, 25 min [MC]: 5 mL of 0.1 M PBS (pH 7.0), room temp [Tran]: QCM (vs SCE), frequency 10 MHz [Regen]: glycine−HCl buffer (ph 2.3), 10 min	[L]: 3−50 ng mL^{-1} [DL]: 1.5 ng mL^{-1} [S]: 4.96 [Re]: six times [CR]: 0.9991	48
[Mat]: Au (QCM) [CM]: folic acid−BSA conjugate [Anal]: folate binding protein (FBP) [MoI]: physical adsorption [IC]: FBP solution [Tran]: QCM	[Det range]: 30−2000 nM	49
[Mat]: APTES/Si-FET [CM]: anti-CEA [BR]: 1% BSA in PBS, pH 8.4, 1 h and 30 min [Anal]: CEA [MoI]: covalent via glutaraldehyde [IC]: (i) CEA in PBS (10 mM, pH 7.4) at various concentrations, 2 h, 20 °C, (ii) 0.76 nM immunogold−anti-CEA in PBS, 2 h [MC]: PBS 10 μM, NaCl 20 μM, pH 7.8 [Tran]: FET, Ac lock-in technique (f = 31.47 Hz, V_{p-p} = 20 mV)	[L]: 0.2−114 ng mL^{-1} [DL]: 0.2 ng mL^{-1}	52
[Mat]: APTES/GMR sensor [CM]: anti-IL-6 [Anal]: three layer, (i) IL-6 and FeCo magnetic particles modified anti-IL-6; two layer, (ii) FeCo magnetic particles modified IL-6 [MoI]: covalent via EDC [Tran]: GMR	[DL]: 20.76 pM (three layer), 373 fM (two layer)	51
[Mat]: in solution [CM]: anti-CEA [Anal]: CEA [DM]: fluorescein isothiocyanate (FITC) labeled secondary antibody [IC]: (i) 10 μL of CEA and 10 μL of 0.2 μg mL^{-1} anti CEA, 45 min, 37 °C, (ii) 20 μL of 0.65 μg mL^{-1} FITC-anti-CEA, 60 min, 37 °C [MC]: 35 mM Tris and 30 mM SDS, pH 9.5 [Tran]: microchip electrophoresis at 3000 V, 80 s	[L]: 60 pg mL^{-1}−8 ng mL^{-1} [DL]: 45.7 pg mL^{-1} [S]: 1.1347 [CR]: 0.9992	18a

biomolecules is crucial. The stability of the materials and matrix has a direct impact on the stability of the biosensor. Various procedures and protocols with a wide variety of matrices like gold nanoparticles (AuNP), AuNP-nanocomposites, sol−gels, layer-by-layer (LBL), self-assembled monolayers (SAM), redox materials, etc., have been used for immobilization of the "capture" biomolecules (Figure 2). Among these materials, use of gold nanoparticles has been explored for binding of antibodies.[34]

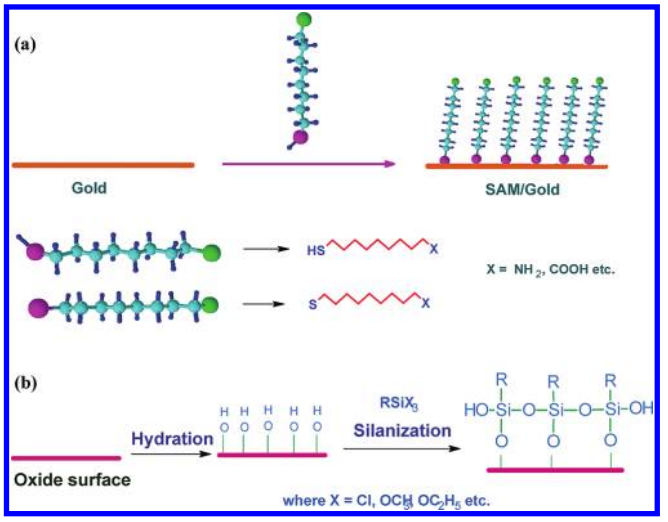

Figure 3. Schematic of (a) thiol SAM and (b) silane SAM formation on gold and oxide surfaces, respectively.

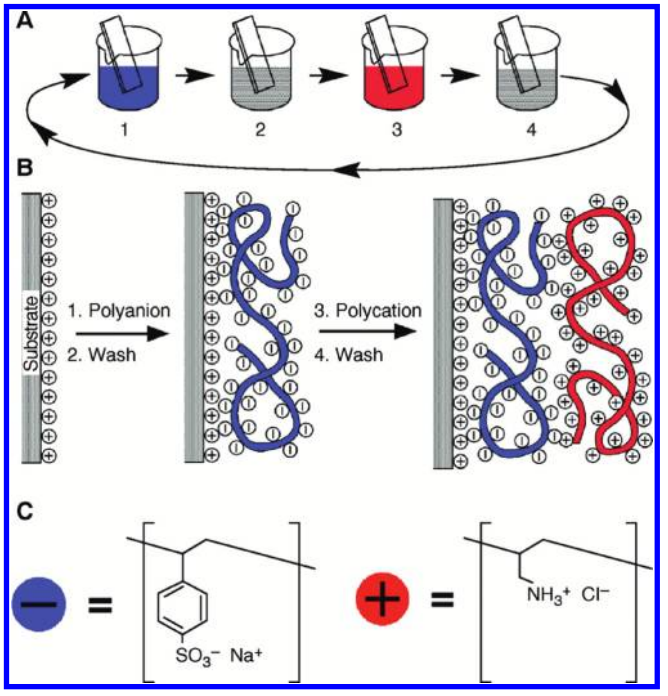

Figure 4. (A) Schematic of the film deposition process using slides and beakers. Steps 1 and 3 represent the adsorption of a polyanion and polycation, respectively, and steps 2 and 4 are washing steps. (B) Simplified molecular picture of the first two adsorption steps. (C) Chemical structures of two typical polyions, the sodium salt of poly(styrene sulfonate) and poly(allylamine hydrochloride). Reprinted with permission from ref 37. Copyright 1997 AAAS.

Along with a larger surface to volume ratio, AuNP exhibit high affinity for proteins and provide a biocompatible environment for antibody binding and act as conductive channels for quick transfer photoinduced electrons at the surfaces of the particles.[35] Researchers have used AuNP and AuNP-nanocomposites in electrode fabrication for direct as well as competitive assay-based estimation of biomarkers.[17b,d−g,i−k,32a] AuNPs have also been

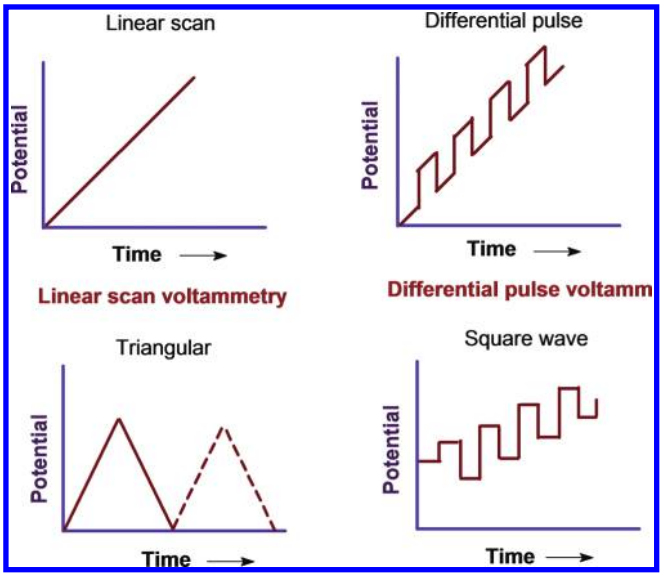

Figure 5. Schematic of potential signal applied with time in voltammetric techniques.

used with SAM and LBL assembly for matrix formation to bind biorecognition molecules in the vicinity of the desired electrode surface.

SAM and LBL techniques result in the formation of ordered organic or inorganic film. SAMs, with a high degree of orientation, molecular order packing, and stability, can be prepared directly on various surfaces using sulfur containing compounds like thiols, dithiols, etc., or using various silanes as illustrated in Figure 3.[36] As illustrated in Figure 4, the LBL self-assembly technique was eloquently described by Decher in 1997.[37] It is a more general and alternative approach for the fabrication of multilayers by consecutive adsorption of anions and cations.[35d] It can be extended to other materials, such as proteins or colloids, and can be used to deposit interesting charged materials such as nanoparticles, conjugated polymers, DNA, proteins, etc., with controlled thickness in nanometer scale. The versatility, ease of preparation, low cost, and potential for scale-up have made SAMs and LBL self-assembly an alternative method in preparing matrices in biosensors.

Other than the above-mentioned matrices, sol−gels and redox complex or polymer-based materials have gained much attention.[17h,l,31a,32b] These provide biocompatible immobilization for the retention of biomolecule activity within the matrix and result in effective electron shuttling between reaction site and electrode surface by means of an electron-hopping process in redox matrix for the fabrication of reagentless biosensors.[38] Researchers have also utilized procedures based on carbon nanoparticles, silica nanowires, membranes, etc., for the binding of biomolecules on the electrode surface for biomarker detection.[17c,21d,32d]

3. ELECTROCHEMICAL TRANSDUCERS FOR LUNG CANCER BIOMARKER DETECTION

As described earlier, electrochemical transduction is based on electrochemical processes taking place at an electrode surface. It involves monitoring of changes of an electrical signal due to an electrochemical reaction at an electrode surface, usually as a

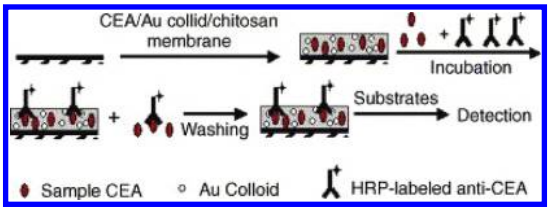

Figure 6. Schematic diagram of the immunoassay procedure used by Wu et al.[17i] Reprinted with permission from ref 17i. Copyright 2006 Elsevier.

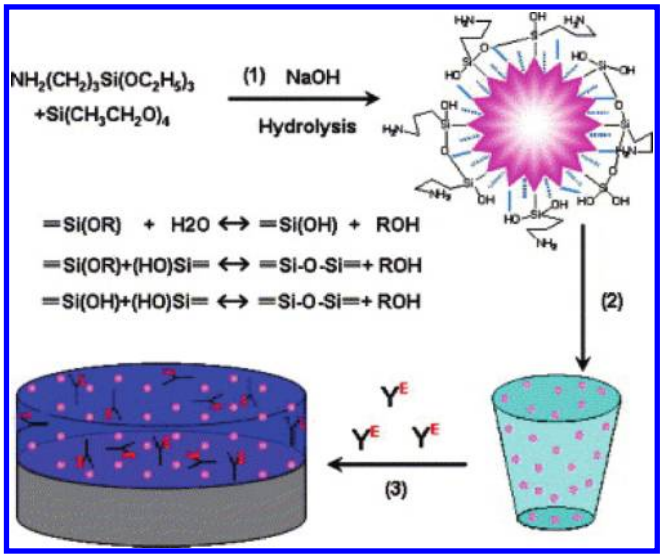

Figure 7. Fabrication procedure of ormosil sol−gel film: (1) hydrolysis of two precursors under weak basic condition, (2) formation of ormosil sol−gel, and (3) preparation of bioactive surface. Reprinted with permission from ref 17h. Copyright 2006 Elsevier.

result of an imposed potential, current, or frequency. Electrochemical biosensors are used in point-of-care devices because they are portable, simple, easy to use, cost-effective, and, in most cases, disposable.[25a] The electrochemical instruments used with the biosensors can be miniaturized to small pocket size devices, which make them applicable for home use. Although amperometric, voltammetric, and potentiometric transducers have been commonly used, voltammetric transducers are preferred for sensitive biomarker detection.

3.1. Voltammetry-Based Biosensors for Lung Cancer Biomarker Detection

In voltammetric techniques, CV and DPV are versatile and the most exploited techniques for lung cancer biomarker detection. CV is becoming an important tool in many areas of chemistry and biochemistry. It is widely used for the study of redox processes and for understanding reaction intermediates. In this technique, potential is varied over a fixed range in a forward and backward direction and current (limited by analyte diffusion at the electrode surface) is monitored (Figure 5). The oxidation and reduction peak current generated during forward and backward scan can be used for analysis.[39] In DPV, potential with a series of fixed amplitude pulses is scanned between initial and final potential. Each succeeding pulse has the same amplitude; however, it starts from a slightly higher base potential (Figure 5). For each pulse, current is measured at just before the application of the pulse and at the end of the pulse, and the difference is estimated and plotted against potential.[39] Other than CV and DPV, LSV and SWV have also been used for lung cancer biomarker detection. LSV is the simplest voltammetric technique, where potential is applied to a working electrode and scanned linearly over the range, and the current is measured (Figure 5).[39a] SWV is a more complex technique, and the excitation signal consists of symmetrical square pulses superimposed on a staircase wave function (Figure 5). SWV has the advantage of higher speed, sensitivity, and rejection of background current.[39b]

3.1.1. Differential Pulse Voltammetry (DPV)-Based Lung Cancer Biomarker Detection. Using DPV technique, various researchers have reported success in fabricating sensitive biosensors for lung cancer biomarkers. Wu et al. reported DPV-based CEA detection using AuNPs/chitosan (CHIT)/screen-printed carbon electrode (SPCE) for entrapment of CEA.[17i] A mixture of thionine (Thi) and hydrogen peroxide (H_2O_2) was used for a competitive assay analysis format with a flow system (Figure 6). The DPV measurements established that the current was inversely propotional to the CEA concentration in the range of 0.50−25 ng mL^{-1}, with acceptable fabrication reproducibility and repeatability. To enhance the response signal, they described a dual-throughput biosensor array for simultaneous determination of CA 19-9 and CA 125 via use of redox active thionine.[21d] Thionine mixed with antigens were physically coimmobilized onto a cellulose acetate membrane, and a competitive bioassay was performed for antigen estimation, in the presence of H_2O_2. Increasing CA 19-9 and CA 125 concentrations resulted in a proportional decrease of catalytic DPV peak currents in the ranges of 0−24 U mL^{-1} and 0−25 U mL^{-1}, respectively. Interassay variation coefficients of 6.4% for 8 U mL^{-1} CA 19-9, and 3% for 13.3 U mL^{-1} CA 125, demonstrated acceptable precision and fabrication reproducibility for sensor. Later, they used AuNP modified horse raddish peroxidase (HRP) labeled antibodies onto the matrix for simultaneous estimation of carcinoma antigen 153 (CA 153), CA 125, and CEA in clinical serum samples.[17j] AuNP modified HRP labeled antibodies were physically entrapped in biopolymer/sol−gel mixed in a 2:1 ratio and drop casted on screen-printed carbon electrodes for bioelectrode fabrication. DPV results indicate the linearity in the ranges of 0.4−140 kU L^{-1}, 0.5−330 kU L^{-1}, 0.8−190 kU L^{-1}, and 0.1−44 μg L^{-1}, with >95.5% positive detection rate for panels of biomarkers of 95 cancer-positive sera cases.

In a similar approach, Du et al. have described the use of CA 19-9 entrapped in titania sol−gel on a graphite electrode for the fabrication of a voltammetric biosensor for CA 19-9 detection.[31a] CA 19-9 trapped in titania sol−gel membrane on graphite electrode was prepared via hydrolysis of adsorbed titanium isopropoxide on the surface of a CA 19-9 drop. Use of titania sol−gel provided the biocompatible microenvironment around the antigen molecule and stabilized its biological activity. Further, antigen down competitive immunoreaction assay was used to avoid labeling reagent for antigen. In the competitive assay, DPV analysis of HRP-catalyzed oxidation of catechol by H_2O_2 reveals linearity over the range of 3−20 U mL^{-1} for CA 19-9 concentrations with a detection limit of 2.68 U mL^{-1}. In another study, use of ormosil containing sol−gel for fabrication of HRP-anti-CEA/sol−gel/graphite electrode has been described by Tan et al.[17h] (Figure 7). Use of an ormosil sol−gel provided the hydrophilic interface for retaining the activity of the bound HRP-anti-CEA. For physically entrapped HRP-anti-CEA, DPV results

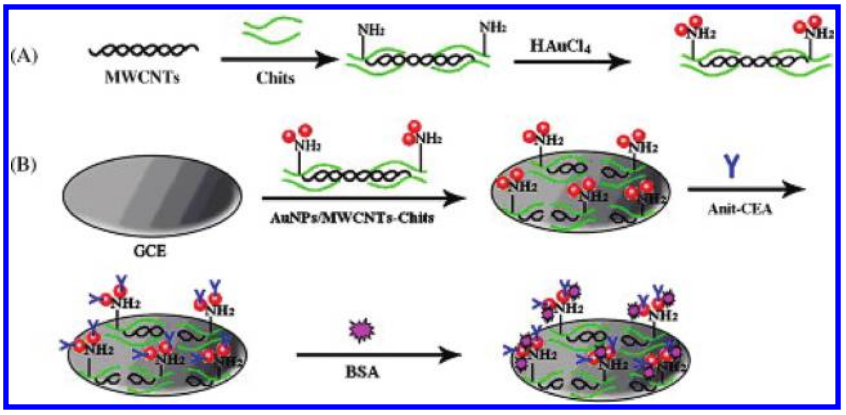

Figure 8. The fabrication procedures for AuNPs/MWCNTs−CHIT composite (A) and the immunosensor (B). Reprinted with permission from ref 17d. Copyright 2010 Elsevier.

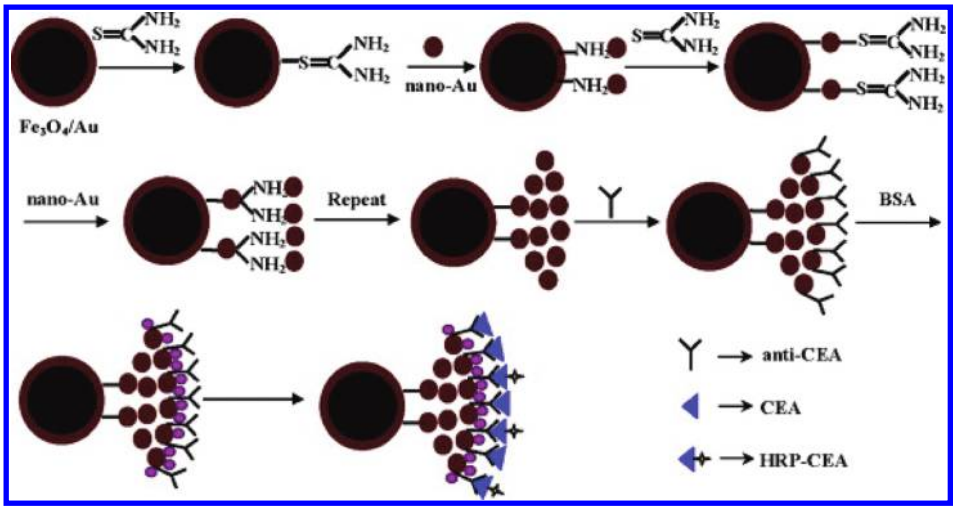

Figure 9. Schematic diagram for the preparation of anti-CEA/nano-Au/Au/Fe_3O_4 nanoparticles and competitive immune reaction. Reprinted with permission from ref 17e. Copyright 2010 Elsevier.

for CEA concentration in serum samples showed two linear ranges 0.5−3.0 and 3.0−120 ng mL^{-1} and good reproducibility. The proposed method was found to be simple and potentially attractive for clinical immunoassays.

For CEA estimation, Lin et al. have proposed an AuNPs−CHIT membrane-based process for electrochemical competitive assay in the presence of *o*-phenylenediamine with H_2O_2.[17g] The HRP-labeled CEA antibodies' interaction response was found to be dependent on immobilization and stability of CEA on the Au-CHIT/ITO. DPV measurements carried out for physically bound CEA showed linearity in the range of 2.0−20 ng mL^{-1} for CEA estimation. Huang et al. described the use of AuNPs in combination with multiwall carbon nanotubes (MWCNTs) for fabrication of anti-CEA/AuNPs/MWCNTs-CHIT/glassy carbon electrode (GCE) by physical adsorption for anti-CEA (Figure 8).[17d] The sensor combines the specificity of the antibodies with the sensitivity of the AuNPs, and MWCNTs amplified electrochemical detection. DPV results reveal linear detection of CEA in two ranges of 0.3−2.5 and 2.5−20 ng mL^{-1}, with a detection limit of 0.01 ng mL^{-1}. In a similar approach using AuNP−nanomaterial composite, Li et al. have described the use of Au/Fe_3O_4 core/shell nanoparticles with AuNPs for competitive assay-based biosensor fabrication (Figure 9).[17e] Physically bound anti-CEA was used to detect CEA in a mixture of HRP-CEA and CEA using DPV in a solution containing hydroquinone and H_2O_2. It was observed that use of a multilayer of nanogold enhanced the specific loading area for antibodies and resulted in the improvement in electron transfer efficiency. Regeneration of the electrode was also easy and achieved by simply removing the magnet and rinsing out all of the magnetic substances on the electrode surface. The biosensor exhibited a detection range of 0.005−50 ng mL^{-1} and stability for 40 days when stored at 4 °C.[17e] Further, using magnetic particles, Fu et al. have proposed a direct and mediator free noncompetitive biosensor for CEA estimation.[40] Results established that use of magnetic particles facilitates easy regeneration and use of HRP blocking in place of bovine serum albumin (BSA) enhances sensitivity. DPV studies indicated a detection limit of 0.5 ng mL^{-1} in the presence of 0.35 mM H_2O_2.

Dai et al. described the use of cysteamine SAM for the fabrication of a thionine/*p*-phthaloyl chloride/cysteamine/Au electrode for CEA estimation in a competitive assay, with H_2O_2 as the detection molecule.[17a] The presence of thionine within the matrix acting as an electron transfer mediator helped to avoid addition of an electron transfer mediator to the solution. However, the procedure lengthened the detection time required due

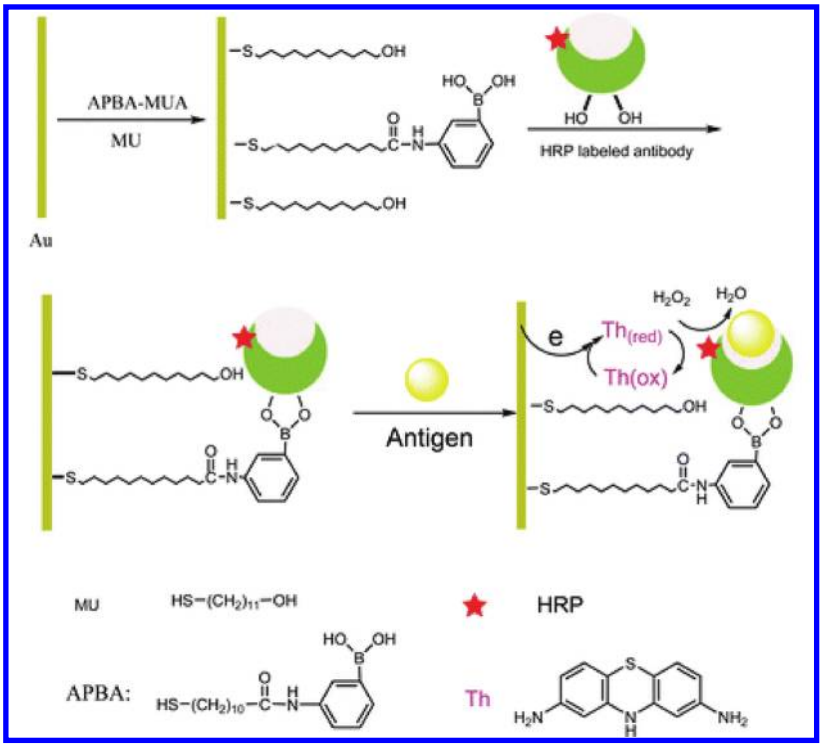

Figure 10. The detection mechanism in using mixed SAM of mercapto undecanol and mercaptoundecanoic acid−phenylboronic acid conjugate-based biosensor. Reprinted with permission from ref 31b. Copyright 2008 The Royal Society of Chemistry.

to an additional elution step of 10 min to elute the HRP-labeled antibody from the wells. Results of the sandwich immunoassay revealed two linear ranges of 0.6−17 and 17−200 ng mL^{-1}, with acceptable precision and reproducibility. In another study, Zhang et al. have shown that for CEA estimation, a biosensor can be fabricated using mixed SAM of mercaptoundecanol and mercaptoundecanoic acid−phenylboronic acid conjugate (Figure 10).[31b] Using physically bound HRP-anti-CEA, CEA was estimated in the presence of H_2O_2. It was observed that in reversible boronic acid−sugar interaction, the formation of the immune complex partially inhibits access of the active center of HRP and thus leads to a linear decrease in the DPV response current for CEA in the concentration range of 2.5−40.0 ng mL^{-1}.

3.1.2. Cyclic Voltammetry (CV)-Based Lung Cancer Biomarker Detection. Cyclic voltammetry (CV) is gaining interest for measurement of analytes in various biosensors and has shown promise for lung cancer biomarker detection. Using the CV technique, Patil et al. have described the application of functionalized Au nanowires for cytokeratin-7 detection.[22d] In a sandwich assay, Au nanowires were used for specific immobilization of biomolecules and found to be effective in improving the sensitivity of the biosensor. Liao et al. described the use of the high affinity of AuNPs for physical adsorption of anti-CEA onto AuNPs assembled on L-cys modified nafion film (Figure 11).[17f] Au nanoparticles on the electrode surface provided a strong and highly stable platform for antibody binding. The biosensor exhibited a linear detection of CEA in the range of 0.01−100 ng mL^{-1}, with a detection limit of 3.3 pg mL^{-1}. Further, Liu et al. used the same property of AuNPs, assembled on organic−inorganic composite film of porous organic material synthesized with 3,4,9,10-perylenetetracarboxylicdianhydride and ethanediamine (PTC-NH_2) on Prussian blue (PB)/GCE electrode surface for

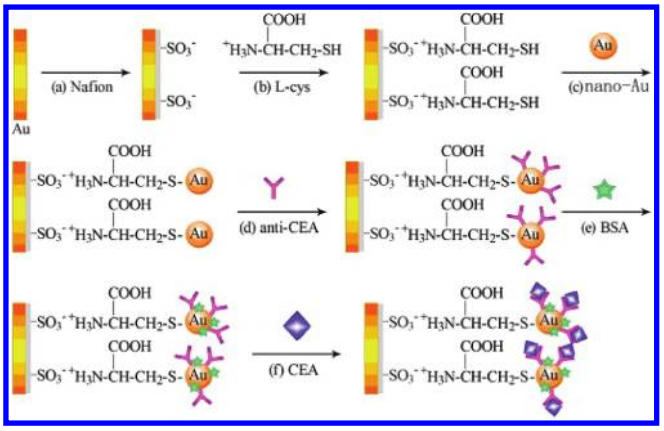

Figure 11. Schematic illustration of the stepwise immunosensor fabrication process: (a) formation of Nf monolayer; (b) adsorption of L-Cys; (c) formation of nano-Au monolayer; (d) anti-CEA loading; (e) blocking with BSA; and (f) incubation with CEA. Reprinted with permission from ref 17f. Copyright 2010 Elsevier.

physical binding of anti-CEA.[32a] Organic−inorganic composite film coupled with an AuNPs-based sensor displayed high sensitivity for CEA detection and exhibited linearity in two ranges of 0.05−2.0 and 2.0−40.0 ng mL^{-1}, with a detection limit of 0.018 ng mL^{-1}. Ou et al. utilized the biocompatibility of AuNPs, MWCNTs, and CHIT with the ease of the LBL technique, to fabricate a label-free biosensor for CEA detection.[35d] LBL self-assembly was done using positively charged AuNPs-MWCNTs-Thi-CHIT composite and polyanionic poly(sodium-*p*-styrenesulfonate) onto a 3-mercaptopropanesulphonic sodium salt (MPS) modified Au electrode. CV results indicated a

dx.doi.org/10.1021/cr100420s |*Chem. Rev.* 2011, 111, 6783–6809

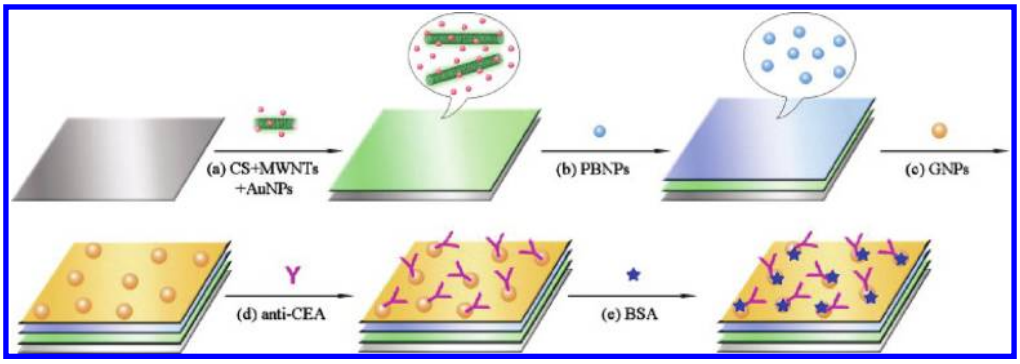

Figure 12. Schematic illustration of the multilayer structured immunosensor fabrication process: (a) fabrication of CS-MWNTs-AuNPs monolayer; (b) absorption of PBNPs; (c) formation of GNPs; (d) adsorption of anti-CEA; and (e) BSA blocking. Reprinted with permission from ref 42. Copyright 2010 Elsevier.

detection limit of 0.01 ng mL^{-1}, with selectivity against human IgG, BSA, alcohol, hepatitis B surface antigen, and glucose. Yuan et al. used AuNPs with $[Ag-Ag_2O]/SiO_2$ nanocomposite for anti-CEA/Au/BSA/$[Ag-Ag_2O]/SiO_2$ nanocomposite/GCE electrode fabrication by physical adsorption of anti-CEA.[17k] In CV studies, peak currents were found to be inversely proportional to the logarithm of CEA concentrations in the range of 0.5−160 ng mL^{-1}. The electrode exhibited selectivity against α-fetoprotein (AFP), BSA, L-cysteine, and human chorionic gonadotropin (HCG) and showed a shelf life of 10 days.

Utilizing biocompatibility of AuNPs and nano-$CaCO_3$ for physical adsorption of anti-CEA, Zhang et al. reported on a reagentless biosensor for CEA detection.[41] Use of these two nanomaterials together helped inhibit the leaking of PB from the electrode surface. CV studies revealed detection limits of 0.1 ng mL^{-1} and easy regenerability using 5 M urea for 5 min. In another study, Zhuo et al. used AuNPs for physical binding of anti-CEA onto a biocatalytic HRP and $Co(bpy)_3^{3+}$/BSA redox biocompatible composite membrane.[32b] The nano-Au/[$Co(bpy)_3^{3+}$/BSA] membrane provided a biocompatible microenvironment for bound antibodies and helped achieve a sensitivity of 0.2858 μA (ng $mL^{-1})^{-1}$ and a linear response to CEA in the 0.50−80.00 ng mL^{-1} range. The sensor was found to be regenerable six times using a Gly−HCl solution. Li et al. described the application of an electrochemically prepared DNA−poly(diallydimethylammonium chloride) (PDDA) polyanion complex membrane with poly (toluidine blue O) and AuNPs, to fabricate a biosensor for CEA detection. Use of the DNA−PDDA membrane enhanced the electrode area and also acted as a charge carrier to facilitate the electron transfer.[35b] Results revealed a sensitivity of 0.106 μA (ng $mL^{-1})^{-1}$ with a shelf life of 1 month. Using an AuNPs/PBNPs/CHIT-MWNTs-AuNPs redox biocompatible composite membrane modified GCE, Song et al. reported the fabrication of a reagentless voltammetric biosensor for CEA estimation (Figure 12).[42] They showed that AuNPs doping in a CHIT−MWNTs composite resulted in enhanced electron transfer, biocompatibility, and helped in physical binding of anti-CEA. Results also demonstrated that the sensor can be regenerated easily in 4 M urea solution and was selective against AFP, CA 125, rat-antihuman CA 15-3, HCG, BSA, L-cysteine, L-glutamate, L-lysine, ascorbic acid, and dopamine. Further, He et al. described the use of an AuNPs/CHIT composite for physical adsorption of anti-CEA onto AuNP/CHIT/nano gold/GCE electrode for CEA estimation.[17b] Results showed a sensitivity of 1310 nA (ng $mL^{-1})^{-1}$ and linearity in the range of 0.2−120.0 ng mL^{-1} for the fabricated electrode. The sensor was found to be regenerable in 4 M urea and exhibited selectivity against AFP, hepatitis B surface antigen, and hepatitis B core antigen, with a long-term stability of 90 days. Liu et al. described an AuNP-porous CHIT-based biosensor for CEA detection and showed that use of porous CHIT helped to improve sensitivity as compared to plain CHIT film.[24f] They attributed this to the fact that the porous structure makes the redox probe more accessible at the electrode surface and provides a larger surface area for the increased amount of antibody loading. Studies in HAc−NaAc buffer showed that the electrodes can be used for detection of CEA up to 0.08 ng mL^{-1} and exhibit selectivity against hepatitis B surface antigen, dopamine, L-cysteine, L-lysine, glucose, and BSA.

To amplify the signal in sandwich assay-based detection, Tang et al. described a biosensor based on thionine-doped magnetic gold nanospheres as the label and HRP as the enhancer for CEA estimation.[34] CV measurements indicated that use of H_2O_2 improved the detection limit from 1.2 to 0.01 ng mL^{-1}, and this was attributed to the catalytic reduction of H_2O_2 by bound HRP. Further, results suggest that thionine doped into bionanospheres acts as a good mediator and facilitates electron transfer. Shi et al. have shown that multilayers of negatively charged AuNPs and positively charged thionine (Thi^+) on pre-electrodeposited nano gold over nano-TiO_2 modified gold surface can be prepared via the LBL technique and can be used for physical binding of anti-CEA in the fabrication of biosensor for CEA detection.[32c] They showed that an amplified current response can be achieved for an electrode by using an HRP backfilling instead of BSA backfilling, which displayed better enzymatic activity to constant concentrations of H_2O_2. With HRP backfilling, the electrode exhibited linearity in the range of 0.2−80.0 ng mL^{-1} as compared to 1.0−80.0 ng mL^{-1} with BSA backfilling. In another study, using LBL assembly of AuNPs and Thi onto nafion modified gold electrode, Yuan et al. proposed a CV-based direct immunosensor for estimation of CEA.[35c] Use of HRP instead of BSA for blocking helped to amplify the signal, and the electrode exhibited a sensitivity of 0.0863 μA (ng $mL^{-1})^{-1}$ with a shelf life of about 45 days when stored at 4 °C. In a similar approach of using HRP as a blocking agent and signal enhancer, Li et al. described the toluidine blue (TB)−polysulfanilic acid (PSAA) modified GCE-based biosensor for CEA estimation (Figure 13).[26] Immobilized HRP helped in amplifying the reduction current response in CV studies of the sensor in PBS containing H_2O_2 with TB as mediator. Results show a detection limit of 0.2 ng mL^{-1} and

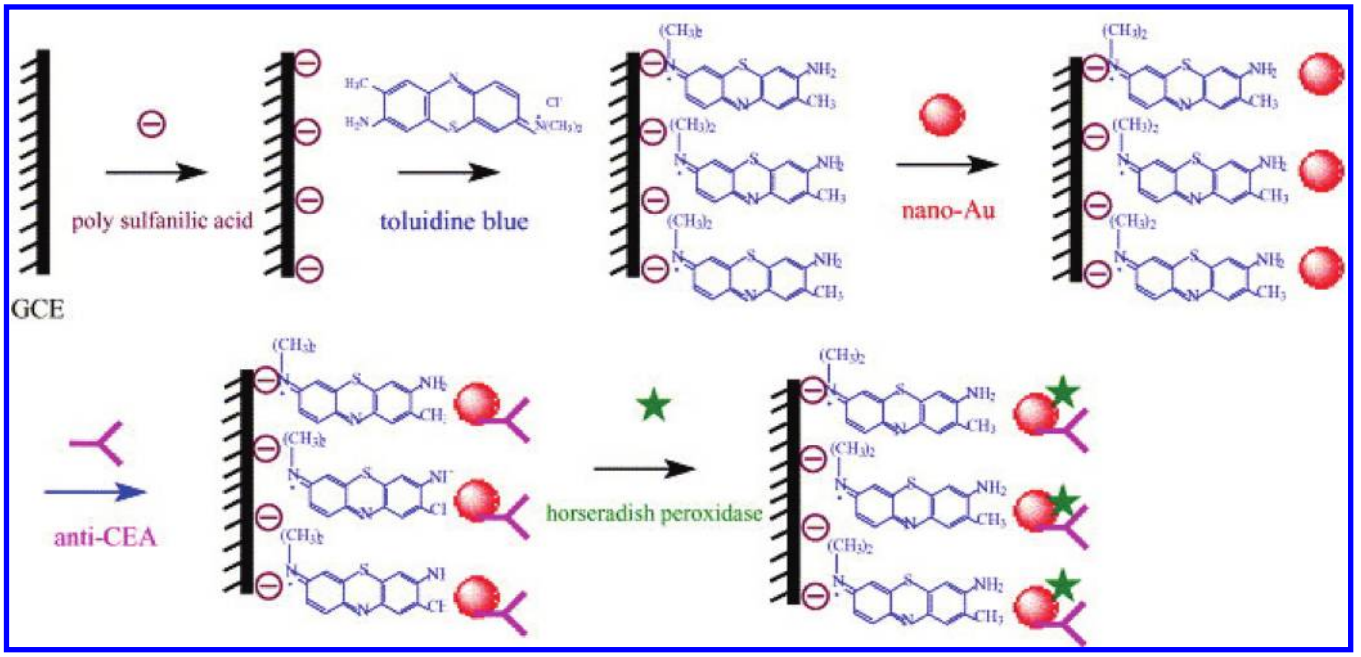

Figure 13. Schematic illustration of the CEA biosensor using toluidine blue (TB)−polysulfanilic acid (PSAA)-modified GCE. Reprinted with permission from ref 26. Copyright 2006 Elsevier.

selectivity against α-fetoprotein and hepatitis B. Zhuo et al. described a reagentless, label-free biosensor based on AuNPs/SiO_2−Thi nanocomposite/AuNPs layers deposited on an electrochemically prepared SAM of Cys on a gold surface.[36b] SiO_2−Thi with AuNPs provided a biocompatible matrix for stable immobilization of anti-CEA and acted as an electrochemical redox probe for reagentless measurement. The electrode exhibited selectivity against various common interferents and was found to be stable for 30 days, with a reusability of seven times when regenerated using 4 M urea.

Utilizing the catalytic properties of Prussian blue (PB) for H_2O_2, Zhong et al. have described an anti-NSE/CHIT/AuNPs/APTES/PB-SiO_2 film on a GCE-based label-free biosensor for NSE estimation.[19b] They showed that the reduction peak current increases significantly upon addition of H_2O_2 to the detection solution, without labeling of enzymes. Results demonstrated a detection limit of 0.08 ng mL^{-1} with selectivity against CEA, CA 125, and progastrin-releasing peptide. In other studies, Ramgir et al. showed that 3-aminopropyltrimethoxysilane (APTMS) silanized silica nanowires can be used for the fabrication of voltammetric biosensor for IL10 and OPN detection.[32d] Results indicated that use of silica nanowires in the presence of *p*-nitrophenyl phosphate helps to achieve detection of IL-10 down to 1 fg mL^{-1} reproducibly.

3.1.3. Linear Sweep Voltammetry (LSV)- and Square Wave Voltammetry (SWV)-Based Lung Cancer Biomarker Detection. Using the LSV technique, Prabhulkar et al. proposed a biosensor for VEGF estimation.[22e] LSV results for a Jeffamine cross-linked ferrocene monocarboxylic acid labeled anti-VEGF onto a carbon fiber micro electrode indicated that formation of immunocomplex causes a decrease in the voltammetric signal of ferrocene carboxylic acid and can be used for VEGF quantification. The electrode exhibited a detection limit of 38 pg mL^{-1} with selectivity against anti-IgG and BSA. In another study, Zhang et al. showed that 3,3′-diaminobenzidine-H_2O_2-HRP can be utilized to fabricate a biosensor for the sensitive detection of CEA.[17l] 3,3′-Diaminobenzidine acted as the electroactive substrate in the HRP-catalyzed oxidation reaction in the presence of H_2O_2 and resulted in production of 4,4′-diimino-bicyclohexylidene-2,5,2′,5′-tetraene-3,3′-diamine, in a Britton−Robinson buffer, which on reduction through a two-electron transfer process gives an electro-reduction peak for measurement of free HRP and labeled HRP. Results of the electrochemical sandwich immunoassay were linear for CEA in the 0.50−80 ng mL^{-1} range.

Using SWV, Ho et al. reported a sandwich assay-based biosensor for ENO1 detection.[20a] Using polyethylene glycol modified SPCE for anti-ENO1 binding, they showed that use of polyethylene glycol not only helped to immobilize the antibody on the electrode surface but also functioned as a stabilizer for antibody binding sites, thus allowing bioprobes to exhibit an improved detection limit of 11.9 fg. Wang et al. described a magnetic approach-based biosensor for CEA estimation.[23c] In a sandwich assay with lead sulphide nanoparticles modified anti-CEA and a secondary antibody, for quantitative measurement using an SWV technique, they achieved a detection limit of 0.5 ng mL^{-1} for CEA. Using anti-CEA tagged ferrocene carboxylic acid encapsulated liposomes (anti-CEA-FCL), Viswanathan et al. reported a voltammetric assay for covalently bound anti-CEA onto polyethyleneimine wrapped MWCNTs on SPE.[33] The magnitude of the SWV peak current for the sandwich immunoassay was found to be proportional to CEA concentration and exhibited a linearity in range of 5×10^{-12}−5×10^{-7} g mL^{-1}, with a detection limit of 1×10^{-12} g mL^{-1} in 0.1 M PBS pH 7.0. In another study, Ho et al. described the use of carbon nanoparticles/polyethyleneimine modified SPGE for covalent binding of anti-CEA.[17c] In a sandwich complex immunoassay with cadmium sulphide nanocrystal quantum dots-based detection of CEA, results of the square wave anodic stripping voltammetry were linear for CEA in the range of 0.032−10 ng mL^{-1} and a detection limit of 32 pg mL^{-1} with a 99.7% level of confidence.

dx.doi.org/10.1021/cr100420s |*Chem. Rev.* 2011, 111, 6783–6809

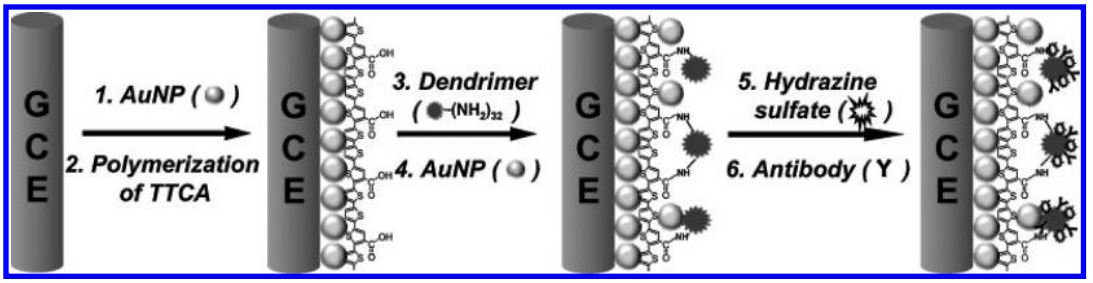

Figure 14. Schematic representation of dendimer-based biosensor fabrication. Reprinted with permission from ref 20b. Copyright 2009 Elsevier.

3.2. Amperometric and Other Electrochemical Techniques-Based Lung Cancer Biomarker Detection

Wilson et al. described an IrO_2 modified glass-based amperometric biosensor for the simultaneous determination of CEA and AFP.[21b] They found no cross-talk between the sensors in the sandwich assay, as the small background responses observed were produced immediately following addition of hydroquinone diphosphate and remained constant throughout the experiments. Also, no cross reactivity was observed between antibodies and nontarget analyte. Results indicated the simultaneous determination of CEA and AFP with detection limits of 1.2 and 1 ng mL^{-1}. Later, they described an IrO_2 modified glass-based amperometric biosensor for simultaneous determination of seven biomarkers and showed that electrochemically grown nanoporous IrO_2 provides a hydrous environment for immobilized proteins and improves efficiency for hydroquinone (HQ) oxidation.[21c]

Tang et al. proposed the electropolymerized poly *o*-aminophenol/Au with AuNP modified anti-CEA onto an Au surface-based biosensor for CEA estimation via label-free EIS technique.[28] They showed that CEA antibody−antigen formation results in an increase of electron transfer resistance of redox probe at the poly *o*-aminophenol/anti-CEA-AuNP/Au electrode and can be used for CEA estimation up to 0.1 ng mL^{-1}. In another EIS-based study, Zhu et al. proposed a direct and simple procedure for CEA estimation.[18c] The electrode was prepared by direct electrochemical deposition of AuNPs on GCE. Results showed that the electrode can be used for estimation of CEA in the 2−80 ng mL^{-1} range with selectivity against AFP, human IgG, complement III; hepatitis B surface antigen; and prostate special antigen. Using a dendimer-based approach, Kim et al. reported a biosensor for Annexin II and MUC5AC estimation (Figure 14).[20b] Electrochemical results indicated that the dendimer-based electrode can sense Annexin II in the 0−0.15 μg mL^{-1} range with a sensitivity of 3140 ± 231.93 Ω (μg mL^{-1})$^{-1}$. Using an external magnet to hold, Pan et al. reported a γ-glycidoxypropyltrimethoxysilane (GPMS) modified $(Fe_3O_4)_{core}-(SiO_2)_{shell}$-based matrix onto a carbon paste electrode (CPE) for fabrication of a label-free EIS immunoassay for CEA estimation.[43] Results indicated that a detection limit of 0.5 ng mL^{-1} can be achieved with easy regeneration simply by magnet removal.

Limbut et al. reported a capacitive biosensor for direct detection of CEA using a thiourea SAM modified electrode.[29a] Their studies demonstrated direct assay of CEA without multiple washing and separation steps. The sensor can be used 45 times for CEA estimation up to 10 pg mL^{-1} with selectivity against AFP. In another study, Lo et al. demonstrated the use of a Ni-decorated single-walled carbon nanotube field effect transistor-based biosensing platform for CEA estimation.[30] They used hexahistidine [$(his)_6$] tagged single chain variable fragments of anti-CEA for sensitive conductometric detection of CEA. Studies showed that use of a Ni-decorated carbon nanotube causes oriented binding of $(his)_6$ tagged single chain variable fragments and thus results in enhanced performance.

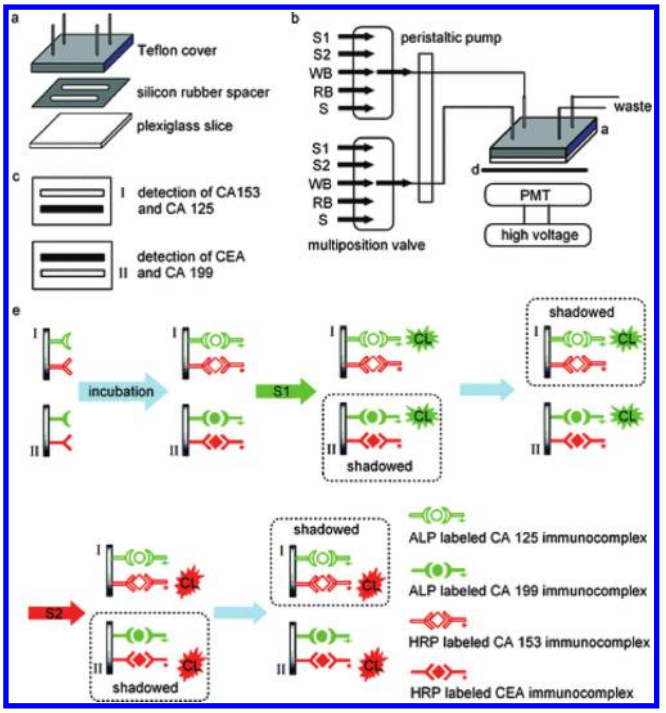

Figure 15. Scheme of the channel and substrate zone two-dimensional resolution system for a multiplex immunoassay of biomarkers panel: (a) flow cell; (b) flow-through system; (c) transect of flow cell for immunoassay; (d) optical shutter; and (e) near-simultaneous multianalyte immunoassay procedure. (S1) ALP substrate, (S2) HRP substrate, (WB) wash buffer, (RB) regeneration buffer, and (S) mixture of sample and tracer antibodies. Reprinted wither permission from ref 44. Copyright 2007 American Chemical Society.

4. OPTICAL TECHNIQUES-BASED LUNG CANCER BIOMARKER DETECTION

Other than electrochemical techniques, various optical techniques have been reported for lung cancer biomarker detection. Fu et al. proposed the chemiluminescent technique-based flow through a sandwich assay system for a substrate zone-resolved multianalyte immunoassay.[24a] Activated aldehydic groups on ultrabinding membrane were used for covalent binding, and *p*-iodophenol (PIP)-luminol-H_2O_2 substrate for CA 125 and

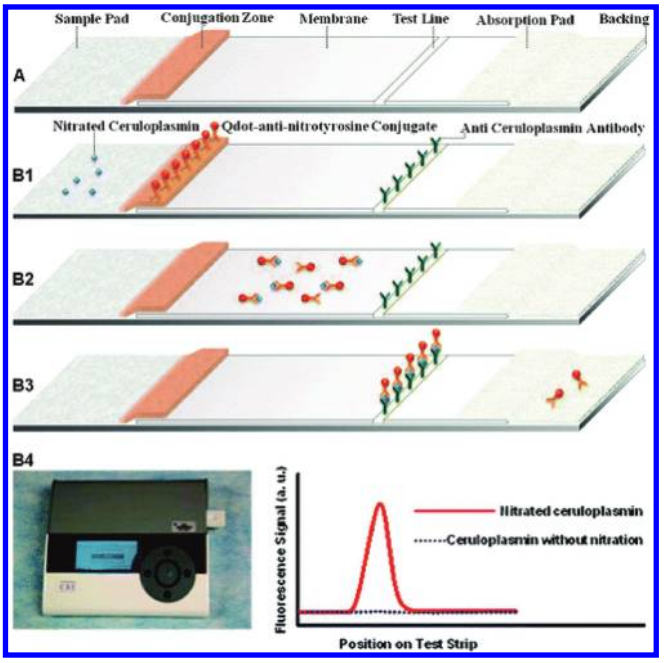

Figure 16. (A) Schematic illustration of the test strip and (B1−B4) the detection of nitrated ceruloplasmin using fluorescent quantum dot-based FLFTS. Reprinted with permission from ref 22f. Copyright 2010 American Chemical Society.

disodium 3-(4-methoxyspiro-(1,2-dioxetane-3,2′-(5′-chloro) tricycle [3.3.1.13,7] decan)-4-yl) phenyl phosphate substrate for CEA were employed for chemiluminescent measurement. It was demonstrated that using this approach, CEA and CA 125 can be detected up to 0.6 ng mL^{-1} and 1.5 U mL^{-1}, respecively. Also, the surface can be easily regenerated for 20 measurements using glycine−HCl. Further, they extended their approach and fabricated two-dimensional resolution devices with a two-channel and substrate zone resolved technique for estimation of CA 125, CA 199, CA 153, and CEA (Figure 15).[44] In another study, Lin et al. described an enzyme immunoassay for CEA via noncompetitive flow injection with chemiluminescent enhancement.[18b] A CEA immunoaffinity column was used for noncompetitive assay, and a mixture of luminal, PIP, and H_2O_2 was employed for signal recording. The electrodes could be reused for up to 30 tests with a detection limit of 0.5 ng mL^{-1}.

A fluorescence-based lateral flow test strip using quantum dots was described by Li et al. for estimation of nitrated ceruloplasmin (Figure 16).[22f] Results showed linear detection in the 1 ng mL^{-1}−10 μg mL^{-1} range, and the test strip was found to be stable for 3 months. Matsumoto et al. described a time-resolved fluoroimmunoassay for simultaneous detection of CEA and AFP.[24c] Using 4,4′-bis(1″,1″,1″,2″,2″,3″,3″-heptafluoro-4″,6″-hexanedion-6″-yl)-chlorosulfo-*o*-terphenyl (BHHCT) tagged Eu^{3+} and Sm^{3+} for AFP and CEA detection, they achieved detection limits of 0.07 ng mL^{-1} for AFP and 0.3 ng mL^{-1} for CEA. In another study, Yan et al. used a flow injection technique with time-resolved fluorescence to describe a flow injection sandwich immunoassay for CEA estimation.[24d] Using Eu labeled anti-CEA, they detected CEA up to 1 ng mL^{-1} in less than 30 min.

Surface plasmon resonance imaging has been used by Li et al. to describe an application of RNA aptamers and antibodies for protein biomarkers detection.[45] Results indicated that in a

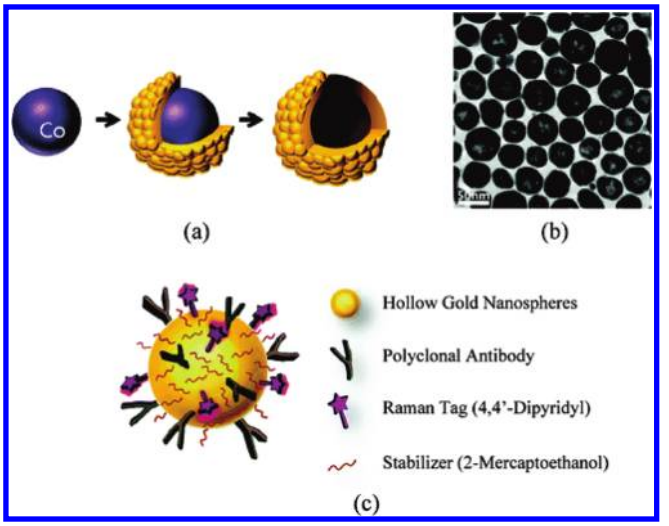

Figure 17. Schematic illustration of HGNs for SERS immunoassay: (a) experimental procedure that generates HGNs by templating against a cobalt nanoparticle, (b) TEM image of HGNs prepared using the template of cobalt nanoparticles, and (c) conjugation of Raman tag (4,4′-dipyridyl) and CEA antibodies onto HGNs. Reprinted with permission from ref 47. Copyright 2009 American Chemical Society.

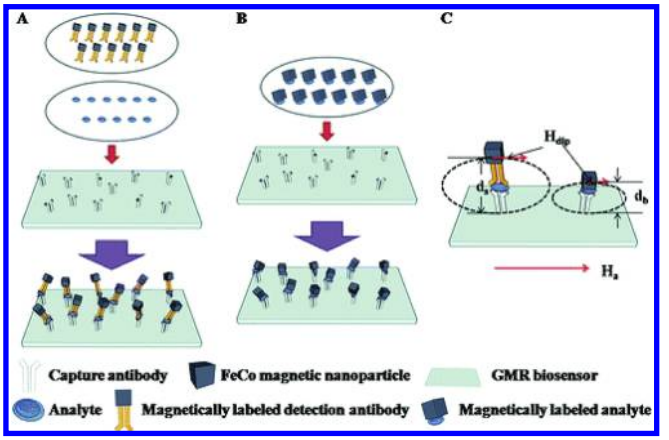

Figure 18. Two GMR sensor and magnetic nanoparticle-based biomolecule detection schemes: (A) three-layer (sandwich) approach, (B) two-layer approach, and (C) GMR biosensor working principle. Reprinted with permission from ref 51. Copyright 2010 American Chemical Society.

sandwich assay with HRP-TMB enzymatically amplified measurements of RNA aptamer microarrays, picomolar concentrations of VEGF protein can be detected. For CEA estimation via SPR, Chung et al. described the application of neutravidin−protein A complex to control the orientation of binding antibodies.[46] In a sandwich assay over oriented antibodies, they achieved a detection limit of 30 ng mL^{-1}. Surface-enhanced Raman scattering (SERS) on hollow gold nanospheres has also been applied for CEA detection (Figure 17).[47] Quantitative analysis using SERS signal at 1612 cm^{-1} demonstrated detection up to 1 pg mL^{-1}.

5. OTHER TECHNIQUES FOR LUNG CANCER BIOMARKER DETECTION

Using AuNP modified (3-mercaptopropyl)trimethoxysilane (MPTS)−hydroxylamine hydrochloride composite, Tang et al.

dx.doi.org/10.1021/cr100420s |*Chem. Rev.* 2011, 111, 6783–6809

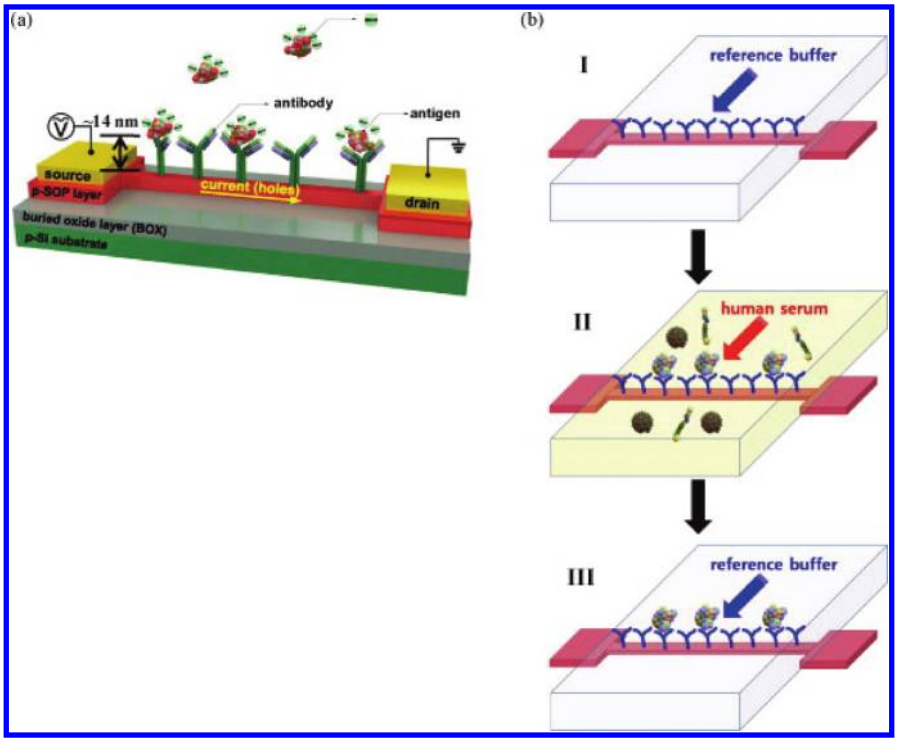

Figure 19. Schematic of the FET-based sensor and new sensing method in physiological solution. (a) FET-based sensor structure immobilized with antibodies and detection of negatively charged antigen and (b) schematic illustration of novel immunodetection using the FET-based sensor in serum. Reprinted with permission from ref 52. Copyright 2010 Elsevier.

described a direct, label-free piezoelectric (quartz crystal microbalance; QCM) immunoassay system for CEA detection.[48] Results showed linearity in 3−50 ng mL^{-1} range with selectivity against CA 125, hepatitis B surface antigen, and human serum albumin. In another study, Henne et al. described the development of a QCM-based biosensor for folate binding protein (FBP) detection.[49] In single step binding, a detection limit of 30 nM was achieved. Further, they showed that with anti-FBP and protein A coated gold nanosphere-based enhancement, detection can be extended up to 50 pM. Using an RT-PCR technique, Sueoka et al. reported the detection of a heterogeneous nuclear ribonucleoprotein B1, mRNA binding protein for early cancer analysis.[50] Results indicated that mRNA in plasma can be used as an effective biomarker for lung cancer detection. Li et al. described the application of a giant megnatoresistive (GMR) sensor for sensitive detection of IL-6.[51] They showed that higher sensitivity can be achieved by use of a two-layer capture technique over a three-layer technique (Figure 18). With the two-layer technique, they achieved the detection limit of 373 fM. Ye et al. described a microchip electrophoresis-based noncompetitive immunoassay technique for CEA estimation.[18a] With their approach, they achieved a detection limit of 45.7 pg mL^{-1}. Using a sandwich assay, Kim et al. reported a field effect transistor-based biosensor (Figure 19) for label-free and real time detection of CEA and achieved a detection limit of 0.2 ng mL^{-1}.[52]

Table 3 gives the details of the matrix used for immobilization [Mat], capturing molecule [CM], method of immobilization [MoI], blocking reagent for nonspecific binding [BR] used for electrode fabrication along with detection molecule [DM], incubation conditions [IC], measurement conditions [MC], regeneration conditions [Regen], and transducer [Tran] used for Analyte [Anal] estimation. Further, it give details of results including linearity [L], detection limit [DL], sensitivity [S], shelf life [SL], reusability [Re], and correlation coefficient [CR] of the various studies made for estimation of lung cancer biomarkers. The table includes the results of electrochemical biosensors with biosensors based on other transduction techniques. It is clear from the table that electrochemical techniques have been the most exploited for lung cancer biomarker detection. Further, it is clear that among electrochemical techniques, DPV and CV techniques allow various strategies to prepare electrodes and result in excellent linearity, sensitivity, detection limits, and other parameters for various lung cancer biomarkers. Moreover, these techniques allow detection of multiple analytes simultaneously with high sensitivity and stability.

6. CONCLUSIONS

It has been shown that various techniques can be utilized with a variety of immobilization matrices for the fabrication of sensitive biosensors for early stage detection of lung cancer biomarkers. Among these, voltammetric techniques provide a general and sensitive approach for direct or multistep measurement for biomarker detection. These methods provide the possibility of simultaneous measurement of various analytes in a short period of time. As the lung cancer biomarker search is gaining momentum for finding new reliable and early stage biomarkers, it is hoped that utilizing the voltammetric technique for simultaneous measurement of various new and more specific lung cancer biomarkers would result in a positive impact on the clinical outcome of lung cancer patients. Further integration of these methods with new nanomaterials and electroactive complexes for electrochemical biosensing will be helpful to enhance the sensitivity and detection limits for newer biomarkers. Also,

the use of an array format for simultaneous measurement with an integrated microfluidic system will provide a solution for reliable early cancer detection and in the fabrication of smart, low-cost, point-of-care devices.

AUTHOR INFORMATION

Corresponding Author

*E-mail: sunilarya333@gmail.com (S.K.A.), bhansali@usf.edu (S.B.).

BIOGRAPHIES

Sunil K. Arya received his B.Sc. in Chemistry in 2002, M.Sc. in Organic Chemistry in 2004, and Ph.D. in Chemistry-Biosensor in 2008 from the University of Delhi, Delhi, India. He is currently a Post Doctorate Fellow in the Department of Electrical Engineering at the University of South Florida. His primary interests are in the development of application of nanomaterials, monolayers, and MEMS for gas sensor and electrochemical biosensor. His research focus is in the areas of micro-/nanofabrication, materials science, and thin film sensors/biosensor.

Shekhar Bhansali received his BE in metallurgical engineering (Honors) from the Malaviya Regional Engineering College (MREC), Jaipur, India (1987), MTech Aircraft Production Engineering from Indian Institute of Technology (IIT), Madras, India, (1991), and a Ph.D. in electrical engineering from the Royal Melbourne Institute of Technology (RMIT), Melbourne, Victoria, Australia (1997). He is currently a professor in the Department of Electrical Engineering at the University of South Florida. His interests are in the areas of Bio-MEMS, nanostructures, energy storage, sensors, and microsystems. He is the recipient of the NSF CAREER award and is also the director of the NSF-IGERT program, a coordinator for Sloan Fellowship Programs, and codirector of NSF Bridges to the Doctorate minority fellowship program. He has over 70 international conference and journal publications and seven pending U.S. patents.

ACKNOWLEDGMENT

This material is partially based upon work supported by the National Science Foundation under Grant No. 0700659.

GLOSSARY

AFP	α-fetoprotein
AuNP	gold nanoparticles
APTES	3-aminopropyltriethoxysilane
CV	cyclic voltammetry
MPS	3-mercaptopropanesulphonic sodium salt
MPTS	3-mercaptopropyltrimethoxysilane
BHHCT	4,4′-bis(1″,1″,1″,2″,2″,3″,3″-heptafluoro-4″,6″-hexanedion-6″-yl)-chlorosulfo-*o*-terphenyl
BSA	bovine serum albumin
CA 125	carcinoma antigen 125
CA 19-9	carbohydrate antigen 19-9
CA 153	carcinoma antigen 153
CEA	carcinoembryonic antigen
CHIT	chitosan
CPE	carbon paste electrode
DPV	differential pulse voltammetry
FCL	ferrocene carboxylic acid encapsulated liposomes
FBP	folate binding protein
HRP	horse raddish peroxidase
HCG	human chorionic gonadotropin
H_2O_2	hydrogen peroxide
LBL	layer-by-layer
LSV	linear sweep voltammetry
MWCNTs	multi walled carbon nanotubes
NSE	neuron-specific enolase
NSCLC	nonsmall cell lung carcinoma
PIP	*p*-iodophenol
PDDA	poly(diallydimethylammonium chloride)
PEG	polyethylene glycol
PA	pulse amplitude
PW	pulse width
PTC-NH_2	3,4,9,10-perylenetetracarboxylicdianhydride and ethanediamine composite
SPCE	screen-printed carbon electrode
SAM	self-assembled monolayer
SCLC	small cell lung carcinoma
SWV	square wave voltammetry
SERS	surface-enhanced Raman scattering
Thi	thionine
VEGF	vascular endothelial growth factor
[Anal]	analyte
[BR]	blocking reagent for nonspecific binding
[CM]	capturing molecule
[CR]	correlation coefficient
[DL]	detection limit
[DM]	detection molecule
[IC]	incubation conditions

[L] linearity
[Regen] regeneration conditions
[Mat] matrix used for immobilization
[MC] measurement conditions
[MoI] method of immobilization
QCM quartz crystal microbalance
[Re] reusability
[S] sensitivity
[SL] shelf life
[Tran] transducer

REFERENCES

(1) (a) Rasooly, A.; Jacobson, J. *Biosens. Bioelectron.* **2006**, *21*, 1851. (b) Tothill, I. E. *Semin. Cell Dev. Biol.* **2009**, *20*, 55. (c) Ullah, M. F.; Aatif, M. *Cancer Treat. Rev.* **2009**, *35*, 193. (d) Wu, J.; Fu, Z. F.; Yan, F.; Ju, H. X. *TrAC, Trends Anal. Chem.* **2007**, *26*, 679.

(2) Sung, H. J.; Cho, J. Y. *BMB Rep.* **2008**, *41*, 615.

(3) (a) Choy, H.; Pass, H. I.; Rosell, R.; Traynor, A. In *Oncology: An Evidence-Based approach*; Chang, A. F., Ganz, P. A., Hayes, D. F., Kinsella, T. J., Pass, H. I., Schiller, J. H., Stone, R. M., Strecher, V. J., Eds.; Springer: New York, 2006. (b) Bharti, A.; Ma, P. C.; Salgia, R. *Mass Spectrom. Rev.* **2007**, *26*, 451.

(4) Marcy, T. W.; Stefanek, M.; Thompson, K. M. *J. Gen. Intern. Med.* **2002**, *17*, 946.

(5) (a) Sutedja, T. G.; Venmans, B. J.; Smit, E. F.; Postmus, P. E. *Lung Cancer* **2001**, *34*, 157. (b) Mazzone, P. J.; Hammel, J.; Dweik, R.; Na, J.; Czich, C.; Laskowski, D.; Mekhail, T. *Thorax* **2007**, *62*, 565.

(6) Brambilla, C.; Fievet, F.; Jeanmart, M.; de Fraipont, F.; Lantuejoul, S.; Frappat, V.; Ferretti, G.; Brichon, P. Y.; Moro-Sibilot, D. *Eur. Respir. J.* **2003**, *21*, 36s.

(7) Soper, S. A.; Brown, K.; Ellington, A.; Frazier, B.; Garcia-Manero, G.; Gau, V.; Gutman, S. I.; Hayes, D. F.; Korte, B.; Landers, J. L.; Larson, D.; Ligler, F.; Majumdar, A.; Mascini, M.; Nolte, D.; Rosenzweig, Z.; Wang, J.; Wilson, D. *Biosens. Bioelectron.* **2006**, *21*, 1932.

(8) (a) Hsu, H. S.; Chen, T. P.; Wen, C. K.; Hung, C. H.; Chen, C. Y.; Chen, J. T.; Wang, Y. C. *J. Pathol.* **2007**, *213*, 412. (b) Ninomiya, H.; Nomura, K.; Satoh, Y.; Okumura, S.; Nakagawa, K.; Fujiwara, M.; Tsuchiya, E.; Ishikawa, Y. *Br. J. Cancer* **2006**, *94*, 1485. (c) Srinivas, P. R.; Kramer, B. S.; Srivastava, S. *Lancet Oncol.* **2001**, *2*, 698.

(9) Herman, J. G. *Chest* **2004**, *125*, 119S.

(10) Greenberg, A. K.; Lee, M. S. *Curr. Opin. Pulm. Med.* **2007**, *13*, 249.

(11) Wang, Y. C.; Hsu, H. S.; Chen, T. P.; Chen, J. T. *Circulating Nucleic Acids Plasma and Serum IV* **2006**, *1075*, 179.

(12) Ganti, A. K.; Mulshine, J. L. *Oncologist* **2006**, *11*, 481.

(13) Kuhn, S. H.; Kock, M. A. D.; Gevers, W. *Chest* **1978**, *74*, 150.

(14) (a) Lin, J. H.; Ju, H. X. *Biosens. Bioelectron.* **2005**, *20*, 1461. (b) Sadik, O. A.; Aluoch, A. O.; Zhou, A. L. *Biosens. Bioelectron.* **2009**, *24*, 2749.

(15) (a) Ocak, S.; Chaurand, P.; Massion, P. P. *Proc. Am. Thorac. Soc.* **2009**, *6*, 159. (b) Chanin, T. D.; Merrick, D. T.; Franklin, W. A.; Hirsch, F. R. *Curr. Opin. Pulm. Med.* **2004**, *10*, 242. (c) Chen, G. A.; Gharib, T. G.; Huang, C. C.; Thomas, D. G.; Shedden, K. A.; Taylor, J. M. G.; Kardia, S. L. R.; Misek, D. E.; Giordano, T. J.; Iannettoni, M. D.; Orringer, M. B.; Hanash, S. M.; Beer, D. G. *Clin. Cancer Res.* **2002**, *8*, 2298.

(16) Tantipaiboonwong, P.; Sinchaikul, S.; Sriyam, S.; Phutrakul, S.; Chen, S. T. *Proteomics* **2005**, *5*, 1140.

(17) (a) Dai, Z.; Chen, J.; Yan, F.; Ju, H. X. *Cancer Detect. Prev.* **2005**, *29*, 233. (b) He, X. L.; Yuan, R.; Chai, Y. Q.; Shi, Y. T. *J. Biochem. Biophys. Methods* **2008**, *70*, 823. (c) Ho, J. A. A.; Lin, Y. C.; Wang, L. S.; Hwang, K. C.; Chou, P. T. *Anal. Chem.* **2009**, *81*, 1340. (d) Huang, K. J.; Niu, D. J.; Xie, W. Z.; Wang, W. *Anal. Chim. Acta* **2010**, *659*, 102. (e) Li, J. P.; Gao, H. L.; Chen, Z. Q.; Wei, X. P.; Yang, C. F. *Anal. Chim. Acta* **2010**, *665*, 98. (f) Liao, Y. H.; Yuan, R.; Chai, Y. Q.; Zhuo, Y.; Yang, X. *Anal. Biochem.* **2010**, *402*, 47. (g) Lin, J. H.; Qu, W.; Zhang, S. S. *Anal. Sci.* **2007**, *23*, 1059. (h) Tan, F.; Yan, F.; Ju, H. X. *Electrochem. Commun.* **2006**, *8*, 1835. (i) Wu, J.; Tang, J. H.; Dai, Z.; Yan, F.; Ju, H. X.; El Murr, N. *Biosens. Bioelectron.* **2006**, *22*, 102. (j) Wu, J.; Yan, F.; Zhang, X. Q.; Yan, Y. T.; Tang, J. H.; Ju, H. X. *Clin. Chem.* **2008**, *54*, 1481. (k) Yuan, Y. L.; Yuan, R.; Chai, Y. Q.; Zhuo, Y.; Mao, L.; Yuan, S. R. *J. Electroanal. Chem.* **2010**, *643*, 15. (l) Zhang, S. S.; Yang, J.; Lin, J. H. *Bioelectrochemistry* **2008**, *72*, 47.

(18) (a) Ye, F. G.; Shi, M.; Huang, Y.; Zhao, S. L. *Clin. Chim. Acta* **2010**, *411*, 1058. (b) Lin, J. H.; Yan, F.; Ju, H. X. *Clin. Chim. Acta* **2004**, *341*, 109. (c) Zhu, Q.; Chai, Y. Q.; Yuan, R.; Wang, N.; Li, X. L. *Chem. Lett.* **2005**, *34*, 1682.

(19) (a) Schneider, J.; Philipp, M.; Velcovsky, H. G.; Morr, H.; Katz, N. *Anticancer Res.* **2003**, *23*, 885. (b) Zhong, Z.; Shan, J.; Zhang, Z.; Qing, Y.; Wang, D. *Electroanalysis* **2010**, *22*, 2569.

(20) (a) Ho, J. A. A.; Chang, H. C.; Shih, N. Y.; Wu, L. C.; Chang, Y. F.; Chen, C. C.; Chou, C. *Anal. Chem.* **2010**, *82*, 5944. (b) Kim, D. M.; Noh, H. B.; Park, D. S.; Ryu, S. H.; Koo, J. S.; Shim, Y. B. *Biosens. Bioelectron.* **2009**, *25*, 456. (c) He, P.; Naka, T.; Serada, S.; Fujimoto, M.; Tanaka, T.; Hashimoto, S.; Shima, Y.; Yamadori, T.; Suzuki, H.; Hirashima, T.; Matsui, K.; Shiono, H.; Okumura, M.; Nishida, T.; Tachibana, I.; Norioka, N.; Norioka, S.; Kawase, I. *Cancer Sci.* **2007**, *98*, 1234. (d) Liu, K.; Shih, N. Y. *J. Cancer Mol.* **2007**, *3*, 45. (e) Kim, S. W.; Cheon, K.; Kim, C. H.; Yoon, J. H.; Hawke, D. H.; Kobayashi, R.; Prudkin, L.; Wistuba, I. I.; Lotan, R.; Hong, W. K.; Koo, J. S. *Cancer Res.* **2007**, *67*, 6565.

(21) (a) Patz, E. F.; Campa, M. J.; Gottlin, E. B.; Kusmartseva, I.; Guan, X. R.; Herndon, J. E. *J. Clin. Oncol.* **2007**, *25*, 5578. (b) Wilson, M. S. *Anal. Chem.* **2005**, *77*, 1496. (c) Wilson, M. S.; Nie, W. Y. *Anal. Chem.* **2006**, *78*, 6476. (d) Wu, H.; Zhang, Z.; Fu, Z. F.; Ju, H. X. *Biosens. Bioelectron.* **2007**, *23*, 114.

(22) (a) Cho, W. C. S. *Biomed. Pharmacother.* **2007**, *61*, 515. (b) Khuri, F. R.; Lotan, R.; Kemp, B. L.; Lippman, S. M.; Wu, H.; Feng, L.; Lee, J. J.; Cooksley, C. S.; Parr, B.; Chang, E.; Walsh, G. L.; Lee, J. S.; Hong, W. K.; Xu, X. C. *J. Clin. Oncol.* **2000**, *18*, 2798. (c) Ma, P. C.; Blaszkowsky, L.; Bharti, A.; Ladanyi, A.; Kraeft, S. K.; Bruno, A.; Skarin, A. T.; Chen, L. B.; Salgia, R. *Anticancer Res.* **2003**, *23*, 49. (d) Patil, S. J.; Zajac, A.; Zhukov, T.; Bhansah, S. *Sens. Actuators, B* **2008**, *129*, 859. (e) Prabhulkar, S.; Alwarappan, S.; Liu, G. D.; Li, C. Z. *Biosens. Bioelectron.* **2009**, *24*, 3524. (f) Li, Z. H.; Wang, Y.; Wang, J.; Tang, Z. W.; Pounds, J. G.; Lin, Y. H. *Anal. Chem.* **2010**, *82*, 7008. (g) Khuri, F. R.; Wu, H.; Lee, J. J.; Kemp, B. L.; Lotan, R.; Lippman, S. M.; Feng, L.; Hong, W. K.; Xu, X. C. *Clin. Cancer Res.* **2001**, *7*, 861. (h) Tang, X. M.; Khuri, F. R.; Lee, J. J.; Kemp, B. L.; Liu, D.; Hong, W. K.; Mao, L. *J. Natl. Cancer Inst.* **2000**, *92*, 1511. (i) Achiwa, H.; Yatabe, Y.; Hida, T.; Kuroishi, T.; Kozaki, K.; Nakamura, S.; Ogawa, M.; Sugiura, T.; Mitsudomi, T.; Takahashi, T. *Clin. Cancer Res.* **1999**, *5*, 1001. (j) Burbee, D. G.; Forgacs, E.; Zochbauer-Muller, S.; Shivakumar, L.; Fong, K.; Gao, B. N.; Randle, D.; Kondo, M.; Virmani, A.; Bader, S.; Sekido, Y.; Latif, F.; Milchgrub, S.; Toyooka, S.; Gazdar, A. F.; Lerman, M. I.; Zabarovsky, E.; White, M.; Minna, J. D. *J. Natl. Cancer Inst.* **2001**, *93*, 691. (k) Yuan, A.; Yang, P. C.; Yu, C. J.; Chen, W. J.; Lin, F. Y.; Kuo, S. H.; Luh, K. T. *Am. J. Respir. Crit. Care Med.* **2000**, *162*, 1957.

(23) (a) Pina, T. C.; Zapata, I. T.; Hernandez, F. C.; Lopez, J. B.; Paricio, P. P.; Hernandez, P. M. *Clin. Chim. Acta* **2001**, *305*, 27. (b) Villena, V.; LopezEncuentra, A.; EchaveSustaeta, J.; MartinEscribano, P.; OrtunodeSolo, B.; EstenozAlfaro, J. *Cancer* **1996**, *78*, 736. (c) Wang, S. F.; Zhang, X.; Mao, X.; Zeng, Q. X.; Xu, H.; Lin, Y. H.; Chen, W.; Liu, G. D. *Nanotechnology* **2008**, 19.

(24) (a) Fu, Z. F.; Liu, H.; Ju, H. X. *Anal. Chem.* **2006**, *78*, 6999. (b) Lin, J. H.; Yan, F.; Hu, X. Y.; Ju, H. X. *J. Immunol. Methods* **2004**, *291*, 165. (c) Matsumoto, K.; Yuan, J. G.; Wang, G. L.; Kimura, H. *Anal. Biochem.* **1999**, *276*, 81. (d) Yan, F.; Zhou, J. N.; Lin, J. H.; Ju, H. X.; Hu, X. Y. *J. Immunol. Methods* **2005**, *305*, 120. (e) Borisov, S. M.; Wolfbeis, O. S. *Chem. Rev.* **2008**, *108*, 423. (f) Liu, Y. X.; Yuan, R.; Chai, Y. Q.; Hong, C. L.; Liu, K. G.; Guan, S. *Microchim. Acta* **2009**, *167*, 217.

(25) (a) Wang, J. *Biosens. Bioelectron.* **2006**, *21*, 1887. (b) Vestergaard, M.; Kerman, K.; Tamiya, E. *Sensors* **2007**, *7*, 3442.

(26) Li, X. L.; Yuan, R.; Chai, Y. Q.; Zhang, L. Y.; Zhuo, Y.; Zhang, Y. *J. Biotechnol.* **2006**, *123*, 356.

(27) Tang, D. P.; Yuan, R.; Chai, Y. Q.; Zhong, X.; Liu, Y.; Dai, J. Y. *Biochem. Eng. J.* **2004**, *22*, 43.
(28) Tang, H.; Chen, J. H.; Nie, L. H.; Kuang, Y. F.; Yao, S. Z. *Biosens. Bioelectron.* **2007**, *22*, 1061.
(29) (a) Limbut, W.; Kanatharana, P.; Mattiasson, B.; Asawatreratanakul, P.; Thavarungkul, P. *Anal. Chim. Acta* **2006**, *561*, 55. (b) Hedstrom, M.; Galaev, I. Y.; Mattiasson, B. *Biosens. Bioelectron.* **2005**, *21*, 41.
(30) Lo, Y. S.; Nam, D. H.; So, H. M.; Chang, H.; Kim, J. J.; Kim, Y. H.; Lee, J. O. *ACS Nano* **2009**, *3*, 3649.
(31) (a) Du, D.; Yan, F.; Liu, S. L.; Ju, H. X. *J. Immunol. Methods* **2003**, *283*, 67. (b) Zhang, X. T.; Wu, Y. F.; Tu, Y. F.; Liu, S. Q. *Analyst* **2008**, *133*, 485.
(32) (a) Liu, Z. Y.; Yuan, R.; Chai, Y. Q.; Zhuo, Y.; Hong, C. L.; Yang, X. *Sens. Actuators, B* **2008**, *134*, 625. (b) Zhuo, Y.; Yuan, R.; Chai, Y. Q.; Sun, A. L.; Zhang, Y.; Yang, J. Z. *Biomaterials* **2006**, *27*, 5420. (c) Shi, Y. T.; Yuan, R.; Chai, Y. Q.; Tang, M. Y.; He, X. L. *J. Electroanal. Chem.* **2007**, *604*, 9. (d) Ramgir, N. S.; Zajac, A.; Sekhar, P. K.; Lee, L.; Zhukov, T. A.; Bhansali, S. *J. Phys. Chem. C* **2007**, *111*, 13981.
(33) Viswanathan, S.; Rani, C.; Anand, A. V.; Ho, J. A. A. *Biosens. Bioelectron.* **2009**, *24*, 1984.
(34) Tang, D. P.; Yuan, R.; Chal, Y. Q. *Anal. Chem.* **2008**, *80*, 1582.
(35) (a) Yang, Z.; Ye, Z.; Zhao, B.; Zong, X.; Wang, P. *J. Sol-Gel Sci. Technol.* **2010**, *54*, 282. (b) Li, N.; Zhao, H.; Yuan, R.; Peng, K.; Chai, Y. *Electrochim. Acta* **2008**, *54*, 235. (c) Yuan, R.; Zhuo, Y.; Chai, Y.; Zhang, Y.; Sun, A. *Sci. China, Ser. B: Chem.* **2007**, *50*, 97. (d) Ou, C. F.; Yuan, R.; Chai, Y. Q.; Tang, M. Y.; Chai, R.; He, X. L. *Anal. Chim. Acta* **2007**, *603*, 205.
(36) (a) Arya, S. K.; Solanki, P. R.; Datta, M.; Malhotra, B. D. *Biosens. Bioelectron.* **2009**, *24*, 2810. (b) Zhuo, Y.; Yu, R. J.; Yuan, R.; Chai, Y. Q.; Hong, C. L. *J. Electroanal. Chem.* **2009**, *628*, 90.
(37) Decher, G. *Science* **1997**, *277*, 1232.
(38) (a) Alqasaimeh, M. S.; Heng, L. Y.; Ahmad, M. *Sensors* **2007**, *7*, 2251. (b) Guschin, D. A.; Sultanov, Y. M.; Sharif-Zade, N. F.; Aliyev, E. H.; Efendiev, A. A.; Schuhmann, W. *Electrochim. Acta* **2006**, *51*, 5137.
(39) (a) Arya, S. K.; Singh, S. P.; Malhotra, B. D. In *Handbook of Biosensors and Biochips*; HH, W., Ed.; John Wiley & Sons: New York; Vol. 1, 2007. (b) Kounaves, S. In *Handbook of Instrumental Techniques for Analytical Chemistry*; FA, S., Ed.; Prentice Hall, Inc.: NJ, 1997.
(40) Fu, X. H. *Biochem. Eng. J.* **2008**, *39*, 267.
(41) Zhang, T. T.; Yuan, R.; Chai, Y. Q.; Liu, K. G.; Ling, S. J. *Microchim. Acta* **2009**, *165*, 53.
(42) Song, Z.; Yuan, R.; Chai, Y.; Yin, B.; Fu, P.; Wang, J. *Electrochim. Acta* **2010**, *55*, 1778.
(43) Pan, J.; Yang, Q. W. *Anal. Bioanal. Chem.* **2007**, *388*, 279.
(44) Fu, Z.; Yang, Z.; Tang, J.; Liu, H.; Yan, F.; Ju, H. *Anal. Chem.* **2007**, *79*, 7376.
(45) Li, Y.; Lee, H. J.; Corn, R. M. *Anal. Chem.* **2007**, *79*, 1082.
(46) Chung, J. W.; Park, J. M.; Bernhardt, R.; Pyun, J. C. *J. Biotechnol.* **2006**, *126*, 325.
(47) Chon, H.; Lee, S.; Son, S. W.; Oh, C. H.; Choo, J. *Anal. Chem.* **2009**, *81*, 3029.
(48) Tang, D. Q.; Zhang, D. J.; Tang, D. Y.; Ai, H. *J. Immunol. Methods* **2006**, *316*, 144.
(49) Henne, W. A.; Doorneweerd, D. D.; Lee, J.; Low, P. S.; Savran, C. *Anal. Chem.* **2006**, *78*, 4880.
(50) Sueoka, E.; Sueoka, N.; Iwanaga, K.; Sato, A.; Suga, K.; Hayashi, S.; Nagasawa, K.; Nakachi, K. *Lung Cancer* **2005**, *48*, 77.
(51) Li, Y. P.; Srinivasan, B.; Jing, Y.; Yao, X. F.; Hugger, M. A.; Wang, J. P.; Xing, C. G. *J. Am. Chem. Soc.* **2010**, *132*, 4388.
(52) Kim, A.; Ah, C. S.; Park, C. W.; Yang, J. H.; Kim, T.; Ahn, C. G.; Park, S. H.; Sung, G. Y. *Biosens. Bioelectron.* **2010**, *25*, 1767.